SDC-92-363

SDC
SOLENOIDAL DETECTOR NOTES

SIMULATION STUDIES OF THE SHOWER MAXIMUM DETECTOR FOR THE SDC: EFFICIENCY FOR THE π^0 REJECTION DEMANDING 90% SINGLE γ RAY

October 21, 1992

J. Grunhaus, S. Kananov and C. Milsténe
TelAviv University

TAUP-2001-92
October 21, 1992

Simulation Studies of the Shower Maximum Detector for the SDC: Efficiency for the π^0 Rejection Demanding 90% Single γ Ray Detection.

J. Grunhaus, S. Kananov, C. Milsténe

School of Physics and Astronomy Raymond and Beverly Sackler Faculty of Exact Sciences TelAviv University, Tel-Aviv 69978, ISRAEL

Abstract

We have demonstrated that π^0 initiated E.M. showers can be efficiently separated from γ ray initiated E.M. showers over a wide range of incident energy, 10 to 80 GeV, using a Shower Maximum Detector (SMD) embedded in the E.M. calorimeter at depths of 5 to $7X_0$. The algorithm which we have developed utilizes two judiciously chosen parameters, the energy weighted radius of the shower, $< R >$ and a parameter which gives a distance weighted measure of the shower energy distribution, as detected by the SMD, ER^2. The separation efficiency is found to be strongly dependent on the incident energy and weakly dependent on the incident polar angle and the energy summation range.

Studies of the dependence of the separation efficiency on segmentation, lead to the interesting and important conclusion that the ideal maximum separation is attained with relatively crude segmentation.

1 Introduction

A Monte Carlo simulation study was carried out to investigate the usefulness of the Shower Maximum Detector (SMD) in the separation of E.M. showers coming from single γ rays from those emanating from π^0's. The SMD was positioned inside the E.M. Calorimeter at two different depths, $5X_0$ and $7X_0$, as measured at polar angle of 90°. For the Monte Carlo studies of the SMD, the E.M. calorimeter was approximated by a mixture of Pb and scintillator (CH) corresponding to a radiation length of 0.8 cm. These studies were done as a function of the segmentation of the SMD, i.e., number of tiles per E.M. calorimeter tower. The Monte Carlo program GEANT 3.14 with an 100 KeV cut for γ's and electrons was used to study E.M. showers in the incident energy range of 10 to 80 GeV. Typically, samples of 200 events were generated for each incident energy point except for the 80 GeV energy point where higher statistics of 300 events were used. The efficiency for the separation of E.M. showers initiated by π^0's from those initiated by γ's was studied for several incident directions. One study was done at the fixed incident direction of $\theta = 75°$ and $\phi = 120°$, while for the second study the incident angles were randomly chosen over an azimuthal range of $\Delta\phi = \pm 1°$ and a polar range of $\Delta\theta = \pm 0.5°$. For the latter study the central value of the azimuthal angle was kept fixed at $\phi = 120°$ and the central value of the polar angle was set in turn to θ=55°, 65°, 75° and 85°. We have used two parameters in order to separate π^0's from single γ rays: the energy weighted radius of the shower measured with the SMD and the 'inertial moment' of the shower energy deposited in the SMD.

2 The Geometry of the Shower Maximum Detector

The geometry of the SMD, proceeding outwardly from the beam line, consists of 2 layers of scintillation (CH) tiles of 0.15 cm thickness. Each scintillator layer consists of a number of equal area tiles which completely cover the cross sectional area of every E.M. tower, as viewed by the incident particle coming from the interaction vertex. The first layer, SMD1, is made up of scintillation tiles giving equal segmentation along the z direction, the beam axis, while the second layer, SMD2, provides equal segmentation in the ϕ direction, also referred to as the x direction. Each tile is individually read out, so the width of the tiles defines the position resolution of the SMD. The

cross sectional area of E.M. towers at a polar angle of 90° approximately equals 11.1 x 10.3 cm^2 so, for instance, a segmentation of the SMD1 into 8 tiles, yields a z position resolution of 1.39 cm, while a similar segmentation of the SMD2 gives a ϕ (x direction) position resolution, of 1.29 cm. The cross section area of the E.M. tower increases as the polar angle decreases so that, for a given segmentation, the z position resolution deteriorates for decreasing value of the polar angle. For an 8 tiles segmentation, the z position resolution at a polar angle of 75° is 1.46 cm and at 55° it is 1.70 cm.

The π^0 rejection efficiency was studied as function of the segmentation of the SMD and simulation calculations were performed for segmentations from 2 through 24 tiles per E.M. tower. Henceforth the tile segmentation of the 2 scintillation layers, SMD1 and SMD2, will be referred to by the notation n_1 x n_2, where n_1 and n_2 denote, respectively, the number of tiles per E.M. tower for the SMD1 and SMD2. We will also use the equivalent notation η x ϕ interchangeably with the notation n_1 x n_2.

The 'Ideal Results' obtainable from an ideal experimental setup having infinitely good position resolution, i.e., $n_1 = \infty$ and $n_2 = \infty$ are shown in the figures and Tables along with the finite segmentation results. It should be pointed out that the Monte Carlo studies presented in this paper are not sensitive to small changes in the thickness of the scintillation tiles.

3 Definition of the Parameters

For every E.M. shower an energy weighted center was calculated, separately, for each of the two scintillation layers. For the SMD1 (z direction) the center of the shower, Z_c was calculated as follows:

$$Z_c = \frac{\Sigma_i Z_i E_i}{\Sigma E_i},$$

where E_i is the energy deposited in the i-th tile and Z_i is the z coordinate of the geometrical center of the i-th tile. The summation is carried out over all the SMD1 tiles having energy deposited. The energy weighted parameter $< R_z >$ was calculated as follows:

$$< R_z > = \frac{\Sigma_i D_i E_i}{\Sigma E_i},$$

where $D_i = \mid Z_i - Z_c \mid$, is the distance along the z direction, of the i-th tile from the calculated center of the shower.

For the SMD2 (ϕ direction) the shower center, X_c, was similarly calculated as follows:

$$X_c = \frac{\Sigma_i X_i E_i}{\Sigma E_i},$$

where E_i is the energy deposited in the i-th tile and X_i is the x coordinate of the geometrical center of the i-th tile. The summation is carried out over all the SMD2 tiles having energy deposited.
The energy weighted parameter $< R_x >$ was calculated as follows:

$$< R_x >= \frac{\Sigma_i D_i E_i}{\Sigma E_i},$$

where $D_i = \mid X_i - X_c \mid$, is the distance along the x, direction of the i-th tile from the calculated center of the shower.

The mean weighted radius, $< R >$, is defined as follows

$$< R >= \sqrt{< R_x >^2 + < R_z >^2}.$$

The second parameter, the 'inertial moment' of the energy deposited in the SMD, ER^2, gives information about the energy structure of the shower. The 'inertial moment' is calculated separately for each layer, and then the sum of the two 'inertial moments' yields;

$$ER^2 = ER_x^2 + ER_z^2,$$

where, $ER_z^2 = \Sigma_i E_i D_i^2$ and $ER_x^2 = \Sigma_i E_i D_i^2$ are, respectively, the 'inertial moments' for SMD1 and SMD2.

4 The Analysis

A careful study of the two above defined parameters, $< R >$ and ER^2, shows that these parameters are useful for the separation of E.M. showers initiated by π^0 's and γ 's.

Scatter-plots of ER^2 versus $< R >$, at 10 GeV incident energy and for the SMD at a depth of $5X_0$ inside the E.M. calorimeter, are shown in Figure 1 for π^0 's and γ's. The γ events shown in Figure 1b, bunch at low $< R >$ and ER^2, while the π^0 events shown in Figure 1a, have relatively higher values of $< R >$ and ER^2. The γ events taper off by $ER^2 \simeq 100$ MeV-cm^2 and $< R >$ value of about 2 cm, whereas the π^0 events reach values of ER^2 up to 500 MeV-cm^2 and $< R >$ up to 4 cm. The difference in the distributions of events in the scatter- plots for the π^0 and γ events facilitates good separation between the E.M. showers initiated by γ's and those initiated by π^0's. Figure 1c shows the overlap of the γ and π^0 scatter-plots.

The following procedure has been devised in order to separate γ E.M. showers from π^0 E.M. showers: a contour was drawn which defines the area in the ER^2 versus $< R >$ γ scatter-plot encompassing 90% of the events. This contour was then copied onto the π^0 ER^2 versus $< R >$ scatter-plot. The π^0 E.M. showers falling within the area defined by the contour contribute to the background of the γ initiated showers, while those falling outside do not contribute to the background. The π^0 rejection efficiency is then given by the ratio of the π^0 events falling outside the area defined by the contour to the sum total of π^0 events. The contour was always chosen to be a rectangle with one side parallel to the x axis, the ER^2 axis, and the second side parallel to the y axis, the $< R >$ axis. The best π^0 rejection efficiency was obtained when minimizing, consistent with 90% γ ray acceptance, the side of the rectangle which is parallel to the y axis.

The π^0 rejection efficiency was studied as a function of the direction and incident energy of the showering particle, the segmentation of the SMD and the summation energy range cut, R_{cut}. A detailed presentation of each of these studies follows.

4.1 Dependence on the Segmentation

The segmentation study was done at 2 incident energies, 10 and 50 GeV and the SMD was positioned at $5X_0$ and $7X_0$ inside the E.M. calorimeter. The results for SMD located at $5X_0$ are shown in Figure 2a and the results for the SMD at $7X_0$ are shown in Figure 2b.

At 10 GeV and SMD at $5X_0$, the π^0 rejection efficiency has a value of $\simeq$56% for the 2 x 2 segmentation, it increases to $\simeq$76% for the 4 x 4 segmentation and it already reaches the 'Ideal Result', as defined in Section 2, of $\simeq$85% for an 8 x 8 segmentation. At 50 GeV a similar behavior is

observed; however, as expected, the overall π^0 rejection efficiencies are lower than those attained at 10 GeV. For an 8 x 8 segmentation a π^0 rejection efficiency of $\simeq$36% is attained while the 'Ideal Result' of $\simeq$44% is reached for a segmentation of slightly more than 16 x 16. The overall performance of the SMD at $5X_0$ and $7X_0$ is similar; however, the π^0 rejection efficiencies at $7X_0$ are higher, for both incident energies, 10 GeV and 50 GeV. It is worthwhile to notice, however, that for the SMD at $7X_0$ the 'Ideal Result' of π^0 rejection efficiency for 10 GeV incident energy of $\simeq$90% is reached for a 20 x 20 segmentation and for 50 GeV incident energy the 'Ideal Result' of $\simeq$56% is not reached by the highest segmentation studied here, 24 x 24.

4.2 Dependence on R_{cut}

The π^0 rejection efficiency is a function of the range over which the energies deposited in the SMD are summed. The amount of energy deposited in the SMD by the showering particles as a function of incident energy is shown in Figure 3a. It turns out that higher π^0 rejection efficiencies are gotten when summing the energy only over a restricted range and not over the whole range. Although the overwhelming bulk of the energy is deposited within short distances of the shower centers, as shown in Figure 3b, the π^0 rejection efficiencies deteriorate when small clusters of energy deposited at relatively large distances from the shower centers, are included in the analysis. It is found that for virtually all E.M. showers the energies deposited in the SMD are confined to $\pm$ 20 cm of the respectively calculated shower centers and, in most of the generated events, within $\pm$ 5 cm. The dependence of the π^0 rejection efficiency on R_{cut} was studied at 3 incident energies, 10, 30 and 50 GeV and 16 x 16 segmentation with the SMD positioned at a depth of $5X_0$. The summation energy range cut, R_{cut}, is defined with respect to the shower centers. The shower centers, Z_c and X_c, are calculated, respectively, by taking the total energy deposited in SMD1 and SMD2, as detailed above in Section 3. The notation, R_{cut}, is then used to denote the energy summation range about the shower centers, i.e., R_{cut} = a cm, denotes an energy summation range of $\pm$a cm about each of the 2 calculated shower centers and 'no R_{cut}' corresponds to the case when all the energy deposited in the SMD was summed over. A weak dependence on R_{cut} is seen in Figure 4 with a maximum π^0 rejection efficiency at $R_{cut} \simeq$ 5 cm for 30 and 50 GeV incident energy while for 10 GeV incident energy the π^0 rejection efficiency increases as a function of increasing R_{cut}, reaching a maximum value of 86$\pm$ 3% with no R_{cut} as seen in Table 2.

E_{in}	SMD at $5X_0$		SMD at $7X_0$	
	R_{cut}=5 cm	no R_{cut}	R_{cut}=5 cm	no R_{cut}
10 GeV	0.80± 0.03	0.86± 0.03	0.76± 0.03	0.83± 0.03
30 GeV	0.71± 0.03	0.67 ± 0.03	0.88 ± 0.03	0.81 ± 0.03
50 GeV	0.54 ± 0.03	0.36 ± 0.03	0.66 ± 0.03	0.44 ± 0.03
80 GeV	0.34 ± 0.02	0.22 ± 0.03	0.47 ± 0.03	0.35 ± 0.03

Table 1: π^0 rejection efficiency for the 8x8 segmentation

E_{in}	SMD at $5X_0$		SMD at $7X_0$	
	R_{cut}=5 cm	no R_{cut}	R_{cut}=5 cm	no R_{cut}
10 GeV	0.82± 0.03	0.86± 0.03	0.79± 0.03	0.87± 0.03
30 GeV	0.81± 0.03	0.77 ± 0.03	0.88 ± 0.03	0.85 ± 0.03
50 GeV	0.57 ± 0.03	0.40 ± 0.03	0.74 ± 0.03	0.48 ± 0.03
80 GeV	0.32 ± 0.02	0.22 ± 0.03	0.53 ± 0.03	0.34 ± 0.03

Table 2: π^0 rejection efficiency for the 16x16 segmentation

4.3 Dependence on Incident Energy

Table 1, shows the π^0 rejection efficiency for 90% γ detection for the 8 x 8 segmentation and the SMD positioned at $5X_0$ and $7X_0$. Table 2 displays the results for the 16 x 16 segmentation.

The π^0 rejection efficiencies for 90% γ detection are compared in Figure 5 for the two different segmentations as a function of incident energy when the SMD is placed at $5X_0$. The Figure 5a displays the results for R_{cut}= 5cm while Figure 5b displays the results for no R_{cut}.Both figures show that the rejection efficiency decreases as a function of incident energy while no significant differences are seen for the two different segmentations. Figure 6 displays the corresponding information when the SMD is placed at $7X_0$. The π^0 rejection efficiency is higher at $7X_0$ than at $5X_0$ for incident energy above 30 GeV. At 10 GeV we observe roughly equal rejection efficiencies for both positions of the SMD.

4.4 The Angular Dependence

The effect, on the π^0 rejection efficiency, of randomly choosing the incident angle of the showering particles within a small cone about a fixed direction, was studied at 10 and 50 GeV incident energy. The results obtained when

E_{in}=10 GeV SMD at $5X_0$	Fixed Angle $\theta = 75°$; $\phi = 120°$		Angular Spread $\theta = 75° \pm 0.5°$ $\phi = 120° \pm 1.0°$		Ideal Results
Segmentation	8 x 8	16 x 16	8 x 8	16 x 16	∞ x ∞
$\bar{E}_d$ by γ (MeV)	41.7± 1.4	41.7± 1.4	42.4± 1.3	42.4± 1.3	42.4± 1.3
$< R >$ for γ (cm)	0.80± 0.04	0.62 ± 0.04	0.82 ± 0.04	0.65 ± 0.04	0.67 ±0.04
ER^2 for γ (MeV cm^2)	37 ± 3	31 ± 3	36 ± 3	30 ± 3	27 ±3
$\bar{E}_d$ by π^0 (MeV)	47± 1.5	47± 1.5	47.9± 1.4	47.9± 1.4	47.9± 1.4
$< R >$ for π^0 (cm)	2.50± 0.09	2.45 ± 0.09	2.60 ± 0.10	2.55 ± 0.10	2.60 ±0.10
ER^2 for π^0 (MeV cm^2)	261±11	250±10	270±12	260±12	270±10
π^0 Rejection	0.86 ± 0.02	0.88 ± 0.02	0.85 ± 0.02	0.86 ± 0.02	0.86±0.02

Table 3: The features of γ and π^0 E.M. showers at 10 GeV and a comparison between the π^0 rejection efficiencies obtained at fixed angle and those gotten for a small angular spread. Results are shown for two segmentations, 8 x 8 and 16 x 16.

keeping the direction of the incoming showering particle fixed at θ= 75° ϕ=120° and those obtained when randomly choosing the incident angle over $\Delta\theta$ =± 0.5° and $\Delta\phi$ = ± 1° about the same fixed angle are shown in Table 3 for 10 GeV and in Table 4 for 50 GeV.

An inspection of Table 3 and Table 4 shows that the effect of randomly choosing the incident direction within a small cone of $\Delta\phi$ x $\Delta\theta \simeq 6{\cdot}10^{-4}$ steradians is not significant. This seemingly not evident result follows from the fact that the 2 parameters used in our analysis, $< R >$ and ER^2 are unaffected by the small angular spread of the incoming showering particles.

We have done a study of the dependence of the rejection efficiency on the direction of the showering particle keeping the azimuthal angle fixed at 120° and varying the central values of the polar angle. The central value of

E_{in}=50 GeV SMD at $5X_0$	Fixed Angle $\theta = 75°$; $\phi = 120°$		Angular Spread $\theta = 75° \pm 0.5°$ $\phi = 120° \pm 1.0°$		Ideal Results
Segmentation	8 x 8	16 x 16	8 x 8	16 x 16	∞ x ∞
$\bar{E}_d$ by γ (MeV)	134 ± 5	134 ± 5	134.6± 4.5	134.6± 4.5	134.6± 4.5
$< R >$ for γ (cm)	0.75± 0.03	0.60 ± 0.03	0.72 ± 0.04	0.64 ± 0.04	0.55 ±0.03
ER^2 for γ (MeV cm^2)	120 ± 8	110 ± 8	120± 8	105 ± 7	94 ±6
$\bar{E}_d$ by π^0 (MeV)	160± 5	160± 5	155.4 ±4.5	155.4± 4.5	155.4± 4.5
$< R >$ for π^0 (cm)	1.00± 0.04	0.93 ± 0.03	1.02 ± 0.06	0.96 ± 0.05	0.94 ±0.03
ER^2 for π^0 (MeV cm^2)	180± 8	170±10	182±10	175± 7	174± 8
π^0 Rejection	0.38 ± 0.03	0.40 ± 0.03	0.36 ± 0.02	0.40 ± 0.03	0.45±0.03

Table 4: The features of γ and π^0 E.M. showers at 50 GeV and a comparison between the π^0 rejection efficiencies obtained at fixed angle and those gotten for a small angular spread. Results are shown for two segmentations, 8 x 8 and 16 x 16.

θ in (Deg)	Numb. of X_0	Pseudo Rapidity	Rejection Efficiency E_{in}=10 GeV 16 x 16	E_{in}=10 GeV ∞ x ∞	E_{in}=50 GeV 16 x 16	E_{in}=50 GeV ∞ x ∞
55	6.1	|0.34|	88 ± 2%	88%	46 ± 2%	48%
65	5.5	|0.07|	86 ± 2%	86%	43 ± 2%	45%
75	5.2	|0.62|	86 ± 2%	86%	40 ± 2%	43%
85	5.0	|1.74|	86 ± 2%	86%	40 ± 2%	42%

Table 5: π^0 Rejection efficiency at 10 and 50 GeV for the 16 x 16 segmentation and the ∞ x ∞ segmentation also referred to as the 'Ideal Results'.

the polar angle was set in turn to θ=55°, 65°, 75° and 85° with the incoming showering particles distributed within a small cone defined by $\Delta\theta = \pm$ 0.5° and $\Delta\phi = \pm$ 1°. The results of a study carried out at 10 GeV and for the SMD situated at $5X_0$, are shown in Figure 7. In Table 5 are shown the number of radiation lengths and pseudo-rapidities for the corresponding values of the angle θ. In the same table the π^0 rejection efficiencies are presented for two different incident energies, 10 and 50 GeV, and for two different segmentations of the SMD, 16 x 16 and ∞ x ∞. At 10 GeV incident energy the rejection efficiency does not show significant dependence on the incident polar angle and for all the angles studied the results are consistent with the 'Ideal Results'. At 50 GeV the π^0 rejection efficiency decreases to about half that attained at 10 GeV and it exhibits a slow inverse dependence on incident angle.

5 General Features of Showers in the SMD

The energy deposited in the SMD at 5 X_0, as a function of incident energy for π^0's and γ's is shown in Figure 3a. The E.M. showers are seen to deposit a maximum of $\simeq$ 0.5% of the total energy in the SMD at 10 GeV, while at 80 GeV they leave only $\simeq$ 0.3% of their total energy. It is noticed that the amount of energy deposited by the π^0 increases relatively to that deposited by the γ ray as the incident energy increases.

The ratio of the energy deposited for R_{cut}= 5 cm to the energy deposited for no R_{cut}, as a function of incident energy, for both π^0's and γ's is shown in Figure 3b. It is interesting to notice that the ratio is close to 1 for the whole energy range, therefore most of the energy is deposited within $\leq| 5cm |$.

The values of $< R >$ as a function of incident energy for γ 's and π^0 's

are shown, respectively, for the 8 x 8 and 16 x 16 segmentations in Figure 8a and Figure 8b.

For incident γ the value of $< R >$ at 10 GeV is $\simeq$0.84 cm for the 8 x 8 segmentation and $\simeq$0.68 cm for the 16 x 16 segmentation. The value of $< R >$ decreases for both segmentations as a function of incident energy reaching $\simeq$0.7 cm for the 8 x 8 segmentation and $\simeq$0.6 cm for the 16 x 16 segmentation at 80 GeV.

For incident π^0 the value of $< R >$ is $\simeq$ 2.5 cm at 10 GeV for both segmentations, it then drops to $\simeq$ 1cm at 30 GeV and thereafter slowly decreases with increasing incident energy. As expected the value of $< R >$ is larger for π^0 than for γ and it is larger at 10 GeV than at 80 GeV.

Detailed studies of $< R >$ for incident γ and π^0 at 10 and 50 GeV, are shown in Figure 9 and Figure 10 as a function of the segmentation for the SMD positioned at $5X_0$ and $7X_0$, respectively.

As the segmentation increases the value of $< R >$ approaches the asymptotic 'Ideal Result'. The expected 'Ideal Result' given by GEANT and shown in the figures are $< R >$=0.67 cm at 10 GeV and $< R >$=0.55 cm at 50 GeV for γ rays and SMD located at $5X_0$ and $< R >$=0.90 cm at 10 GeV and $< R >$=0.68 cm at 50 GeV for SMD located at $7X_0$.

For incident π^0 the 'Ideal Result' is $< R >$=2.6 cm at 10 GeV and $< R >$=0.95 cm at 50 GeV for the SMD located at $5X_0$, and for the SMD located at $7X_0$ $< R >$=2.5 cm at 10 GeV and $< R >$=0.99 cm at 50 GeV. In the energy range that we have studied, we find that the value of $< R >$ is sensitive to the depth at which the SMD is placed inside the E.M. calorimeter for π^0 initiated showers and rather insensitive for the case of γ initiated showers. With increasing segmentation, the values of $< R >$ converge fairly rapidly to the values of the 'Ideal Result'.

The ER^2 parameter was studied as a function of incident energy for π^0 's and γ's. Two segmentations were considered in this study, 8 x 8 and 16 x 16. The results shown in Figure 11a and Figure 11b, correspond, respectively, to γ and π^0 initiated E.M. showers, with the SMD located at $5X_0$. The results for incident γ rays shown in Figure 11a display a monotonic increase in the value of ER^2 as a function of incident energy. The values for the 8 x 8 segmentation are consistently higher than those for the 16 x 16 segmentation. For incident π^0, the parameter ER^2 has a maximum value of $\simeq$ 300 MeV-cm^2 at 10 GeV, decreases to a value of $\simeq$ 160 MeV-cm^2 at 30 GeV and then increases to a value of $\simeq$ 200 MeV-cm^2 at 80 GeV. This behavior ensues since the π^0 initiated shower is made up of a superposition of two γ ray initiated showers which are angularly separated by the opening

angle of the $\pi^0 \rightarrow 2\ \gamma$ decay. With increasing incident energy the opening angle decreases thereby decreasing the value of ER^2 as seen when the energy increases from 10 to 30 GeV. At the same time the contribution of each of the 2 γ, by themselves, to the value of ER^2 increases monotonically, as seen In Figure 11a. Above 30 GeV, the monotonic increase of ER^2 for each of the γ's dominates over the effect of the decreasing opening angle, thereby causing the value of ER^2 to increase as seen in Figure 11a. As expected, the values of ER^2 for incident π^0 are consistently higher, over the whole energy range, than the corresponding incident γ ray values.

The value of ER^2 was studied as a function of segmentation at two incident energies, 10 and 50 GeV. Results for incident π^0's and γ rays for the SMD positioned at $5X_0$ are displayed in Figure 12 while Figure 13 shows the results for the SMD positioned at $7X_0$. The 'Ideal Results', as given by GEANT for infinitely fine segmentation, are indicated in the figures. Both the π^0 and γ results show a clear dependence on segmentation; however, the dependence is more pronounced at 50 GeV. The 'Ideal Results' are reached for both incident energies at a segmentation of 20, for the SMD at $5X_0$, and at 16, for the SMD at $7X_0$.

6 Conclusions

It has been demonstrated that π^0 initiated E.M. showers can be efficiently separated from γ ray initiated E.M. showers over a wide energy range, 10 to 80 GeV, using an analysis based on two judiciously chosen parameters, $< R >$ and ER^2. The results of this analysis are weakly dependent on R_{cut} and on the incident polar angle.

The π^0 rejection efficiency is found to be strongly dependent on the incident energy, it is $80 \pm 3\%$ at 10 GeV and decreases to $38 \pm 2\%$ at 80 GeV for the SMD located at $5X_0$ and R_{cut}= 5cm. For incident energy above 30 GeV, the π^0 rejection efficiency is higher for the SMD located at $7X_0$, while at 10 GeV the SMD positioned at $5X_0$ gives better π^0 rejection. Studies of the dependence of the π^0 rejection efficiency on segmentation, lead to the interesting and important conclusion that the maximum π^0 rejection efficiency, the 'Ideal Results', are attained with relatively crude segmentation. For the SMD at $5X_0$ and 10 GeV incident energy the 'Ideal Results' are reached with an 8 x 8 segmentation and similarly an $\simeq$ 18 x 18 segmentation suffices for 50 GeV incident energy.

List of Figures

1 The scatter plots of ER^2 versus $< R >$ for 10 GeV showering particles. The SMD is located at $5X_0$: a) for showering π^0's a nd b) for showering γ's. The conto ur which demarcates the γ initiated shower region is shown. c) Is a superposition of a) and b). . . . . .

2 The π^0 rejection efficiency for 90% γ detection efficiency as a function of the segmentation for 10 and 50 GeV incoming energies. a) SMD locat ed at $5X_0$ and b) SMD located at $7X_0$.

3 a)The energy deposited in the SMD by showering π^0's and γ's (in MeV) as a function of the incident energy (in GeV). SMD is located at $5X_0$ and R_{cut} = 5 cm and b) the ratio of the dep osited energy in the SMD for R_{cut}=5cm to the deposited energy for no R_{cut}, as a function of the incident energy. . . .

4 The π^0 rejection efficiency for 90% γ detection efficiency as a function R_{cut} for the 16x16 segmentation, for 3 different π^0 incomi ng energies 10, 30 and 50 GeV. . . . . .

5 The π^0 rejection efficiency for 90% γ detection efficiency as a function of the incident energy for two different SMD segmentations, 8 x 8 and 16 x 16. The SMD is located at a depth of 5 X_0 inside the E.M. Calorimeter. a) For R_{cut} = 5 cm and b) for no R_{cut}. . . . . .

6 The π^0 rejection efficiency for 90% γ detection efficiency as a function of the incident energy for two different SMD segmentations, 8 x 8 and 16 x 16. The SMD is located at a depth of 7 X_0 inside the E.M. Calorimeter. a) For R_{cut} = 5 cm and b) for no R_{cut}. . . . . .

7 The π^0 rejection efficiency as a function of the polar angle θ for the SMD located at $5X_0$ and 10 and 50 GeV incoming energies. The dashed and dot-dashed lines represent, respectively, th e 'Ideal Results' at 10 and 50 GeV. . . . . .
8 The values of $< R >$ as a function of incident energy are shown for the 8 x 8 and 16 x 16 segmentations for no R_{cut} and SMD located at $5X_0$: a) for sho wering γ 's and b) for showering π^0's . . . . . .
9 The values of $< R >$ for showering particles at 10 and 50 GeV as a function of the segmentation. The SMD located at $5X_0$: a) for showering γ 's and b) for showering π^0's. . . . . .
10 The values of $< R >$ for showering particles at 10 and 50 GeV as a function of the segmentation. The SMD located at $7X_0$: a) for incoming γ 's and b) for incoming π^0's. . . . . .
11 The values of ER^2 as a function of incident energy are shown for the 8 x 8 and 16 x 16 segmentations with no R_{cut} and SMD located at $5X_0$: a) for showering γ 's and b) for showering π^0's.
12 The values of ER^2 for showering particles at 10 and 50 GeV as a function of the segmentation. The SMD is located at $5X_0$: a) for incoming γ 's a nd b) for incoming π^0's. . . . .
13 The values of ER^2 for showering particles at 10 and 50 GeV as a function of the segmentation. The SMD is located at $7X_0$: a) for incoming γ 's an d b) for incoming π^0's. . . . . .

SMD at 5 RL for incoming π^0 and γ at 10 GeV

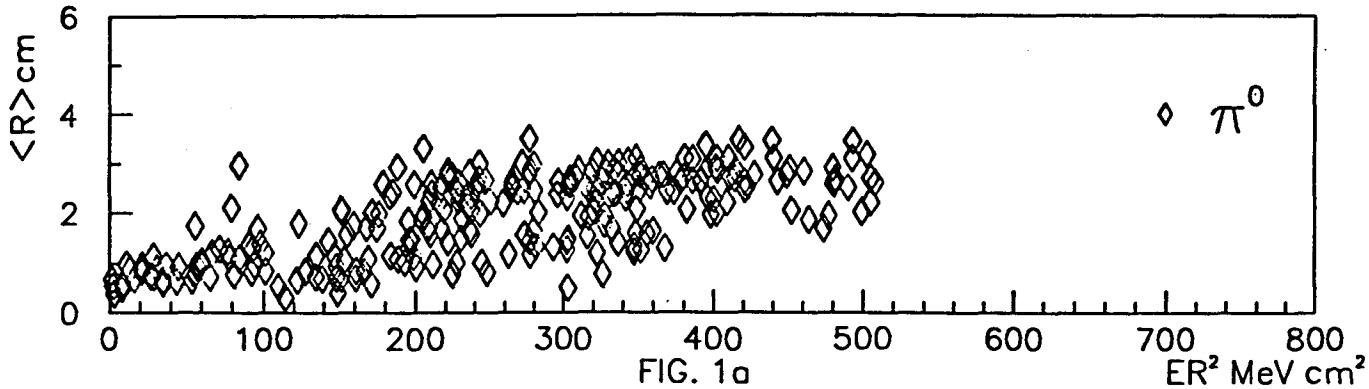

FIG. 1a

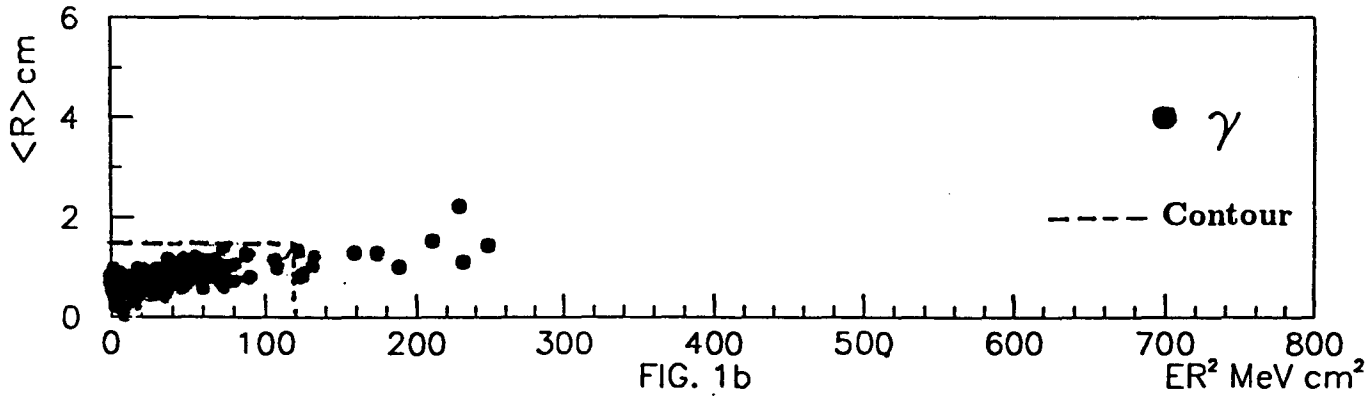

FIG. 1b

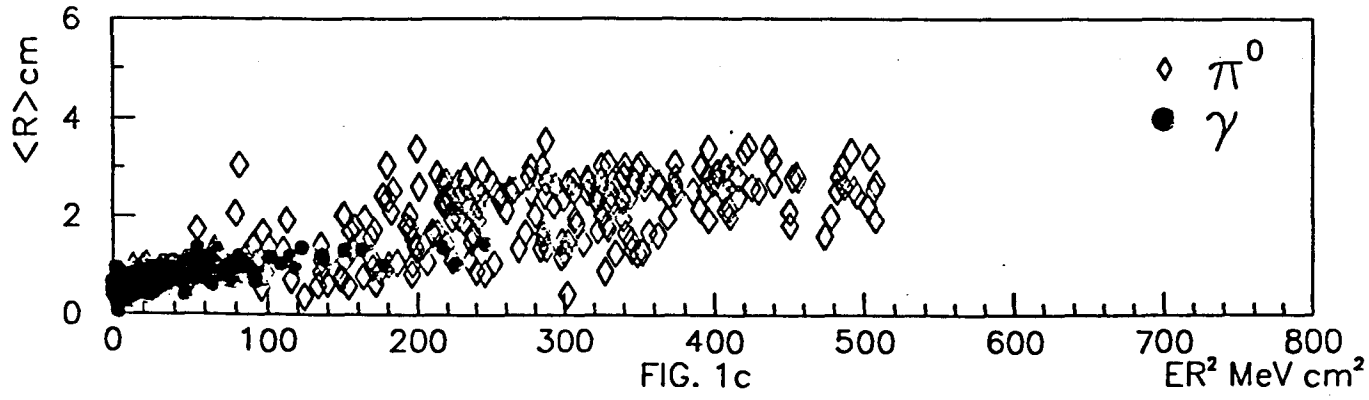

FIG. 1c

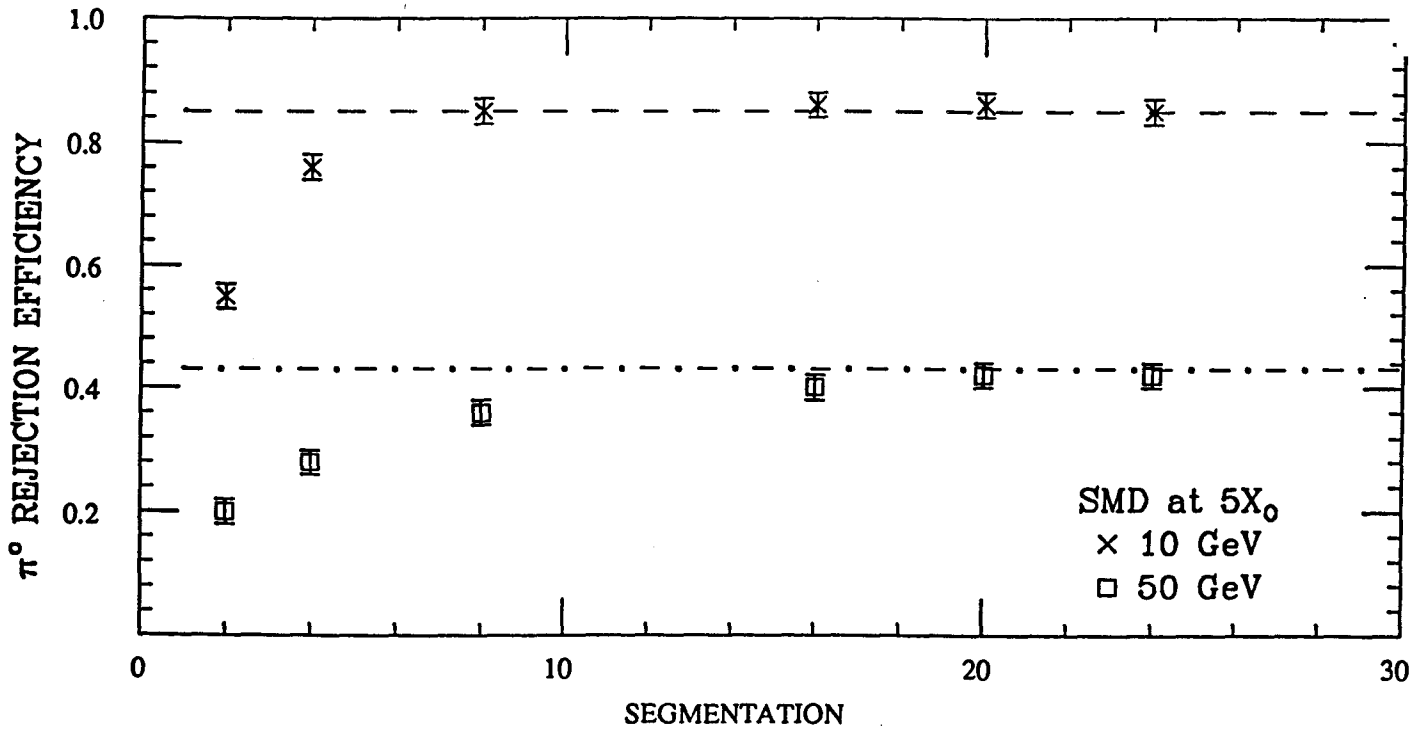
1.0
0.8
0.6
0.4
0.2
π° REJECTION EFFICIENCY
0
10
20
30
SEGMENTATION
SMD at 5X₀
× 10 GeV
□ 50 GeV

FIG.2a

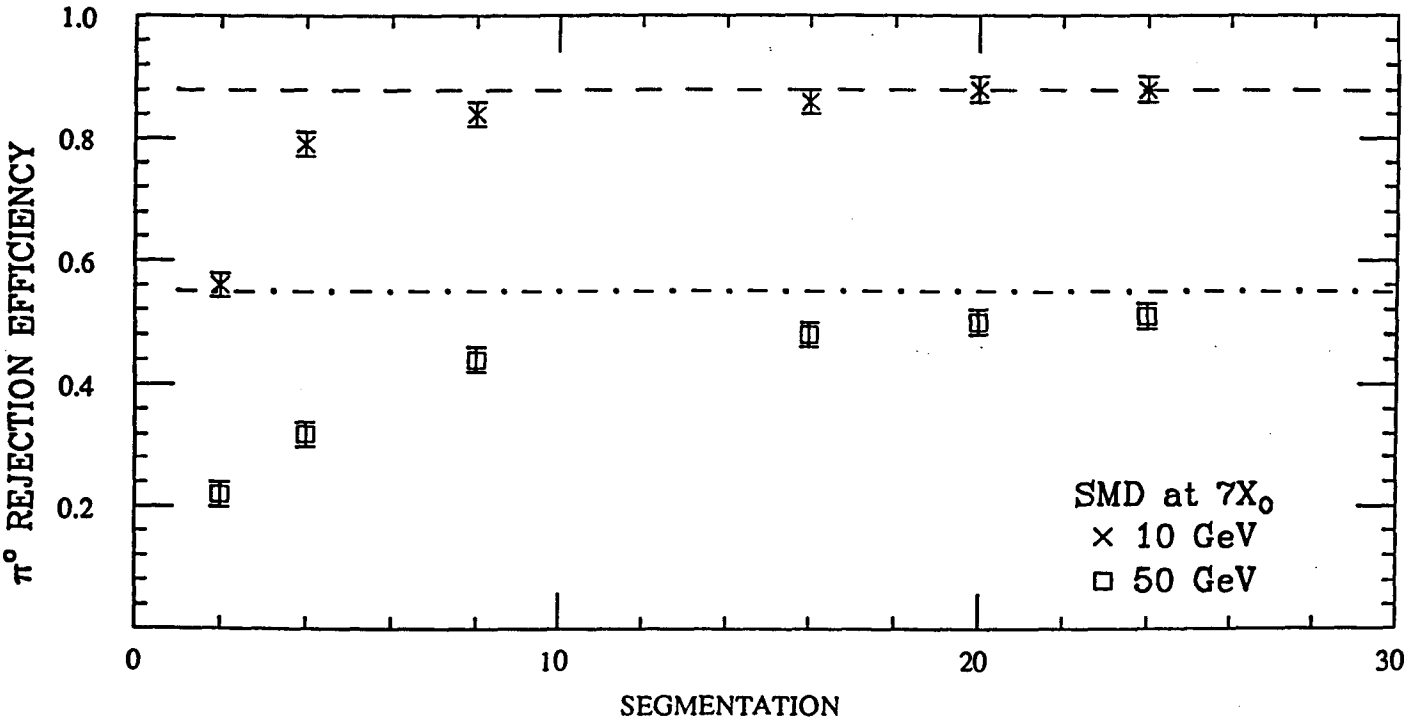
1.0
0.8
0.6
0.4
0.2
π° REJECTION EFFICIENCY
0
10
20
30
SEGMENTATION
SMD at 7X₀
× 10 GeV
□ 50 GeV

FIG.2b

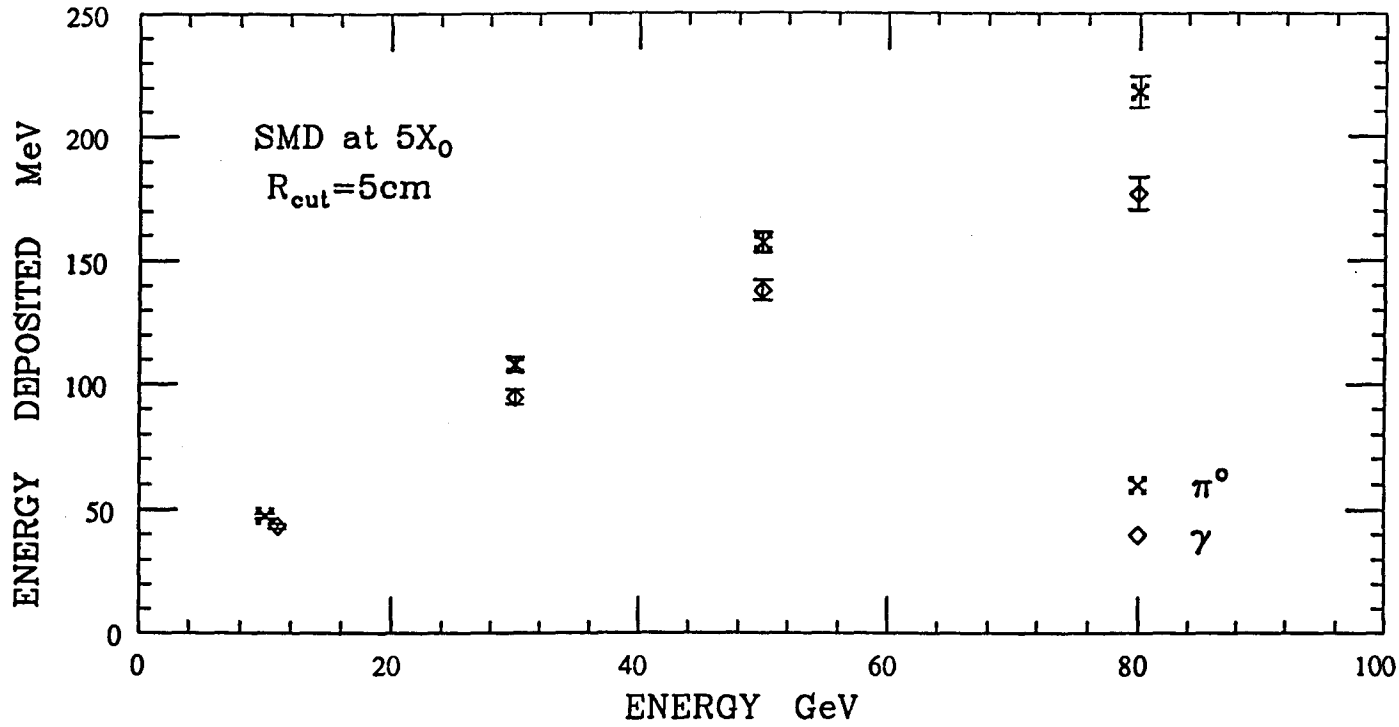
SMD at 5X0
Rcut=5cm
ENERGY DEPOSITED MeV
ENERGY GeV
π°
γ
0
50
100
150
200
250
0
20
40
60
80
100

FIG.3a

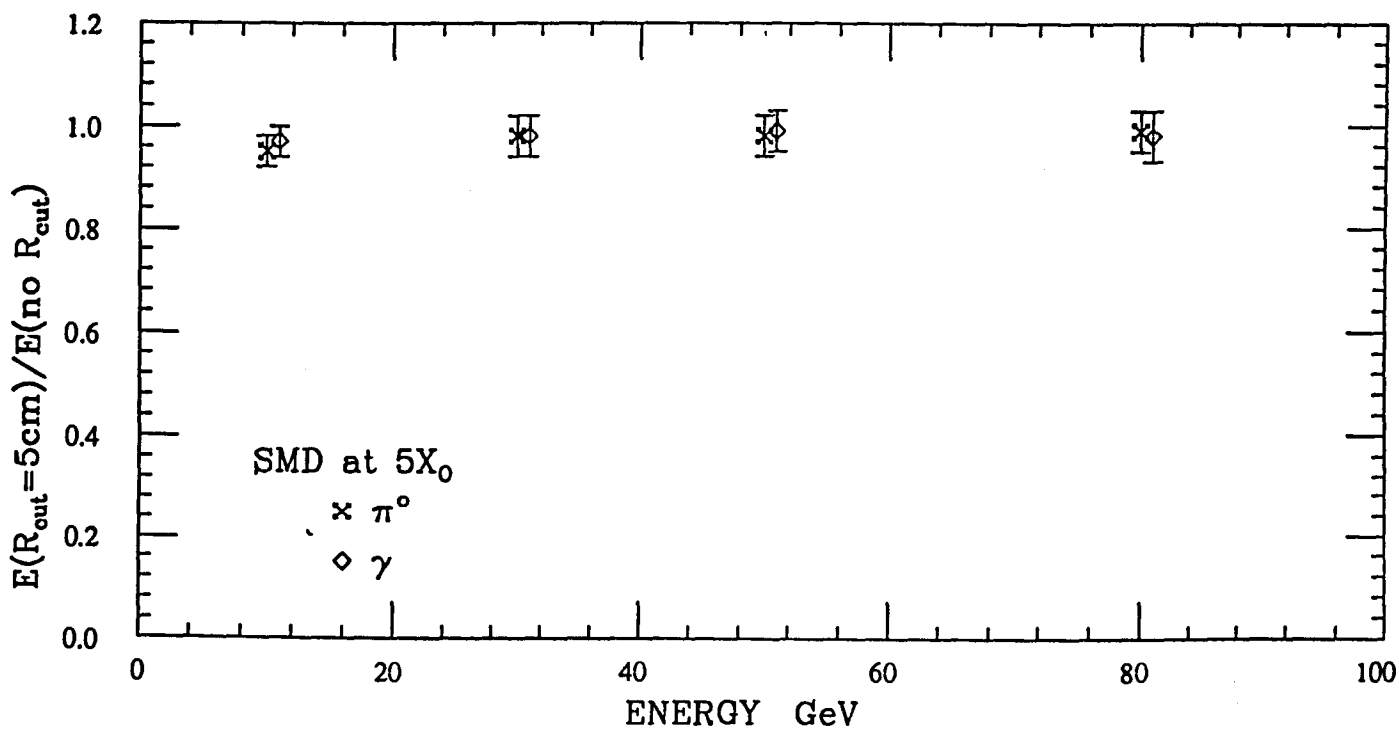
SMD at 5X0
π°
γ
E(Rcut=5cm)/E(no Rcut)
ENERGY GeV
0.0
0.2
0.4
0.6
0.8
1.0
1.2
0
20
40
60
80
100

FIG.3b

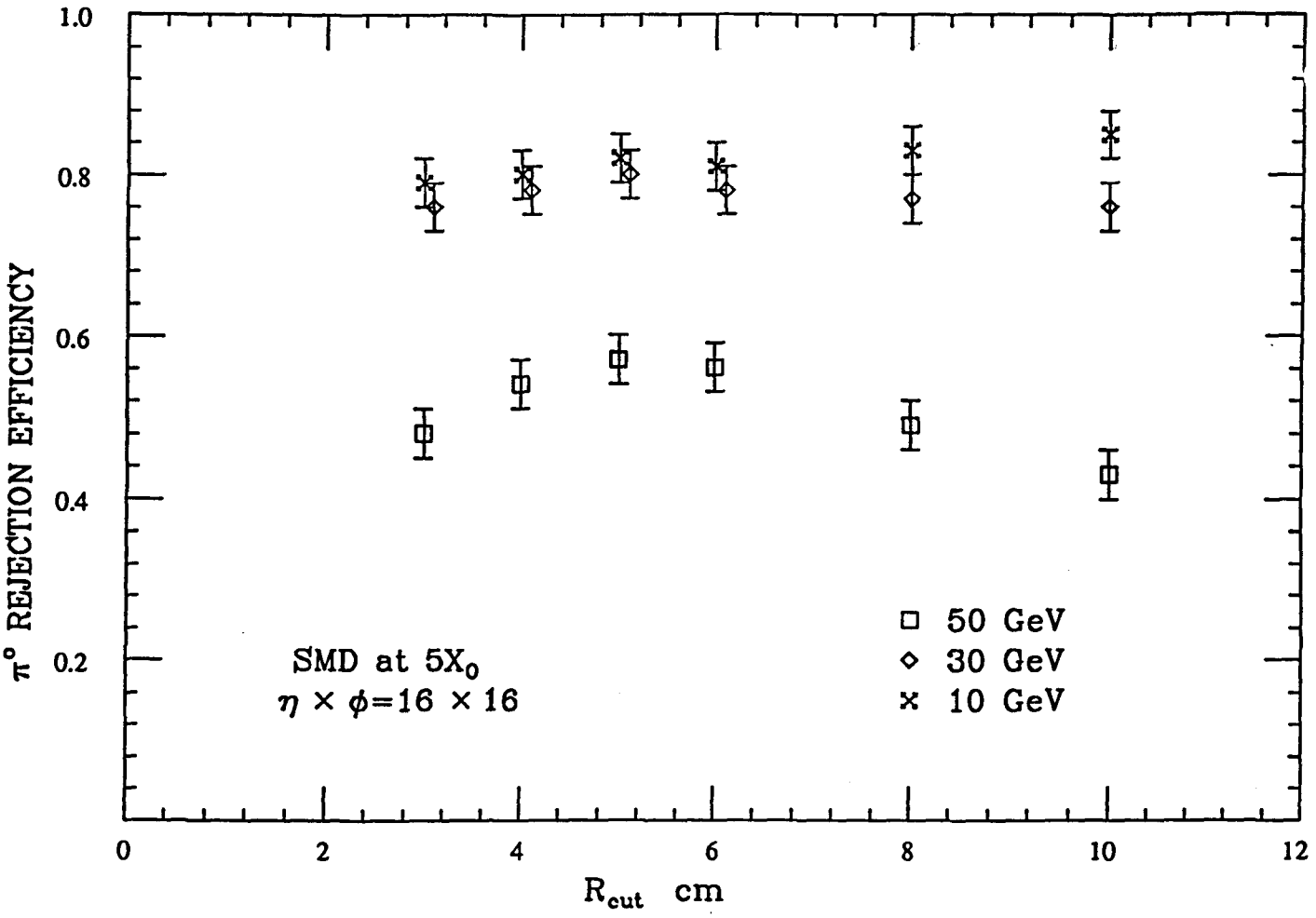
1.0
0.8
0.6
0.4
0.2
π^o REJECTION EFFICIENCY
SMD at $5X_0$
$\eta \times \phi$=16 × 16
50 GeV
30 GeV
10 GeV
0
2
4
6
8
10
12
R_{cut} cm

FIG.4

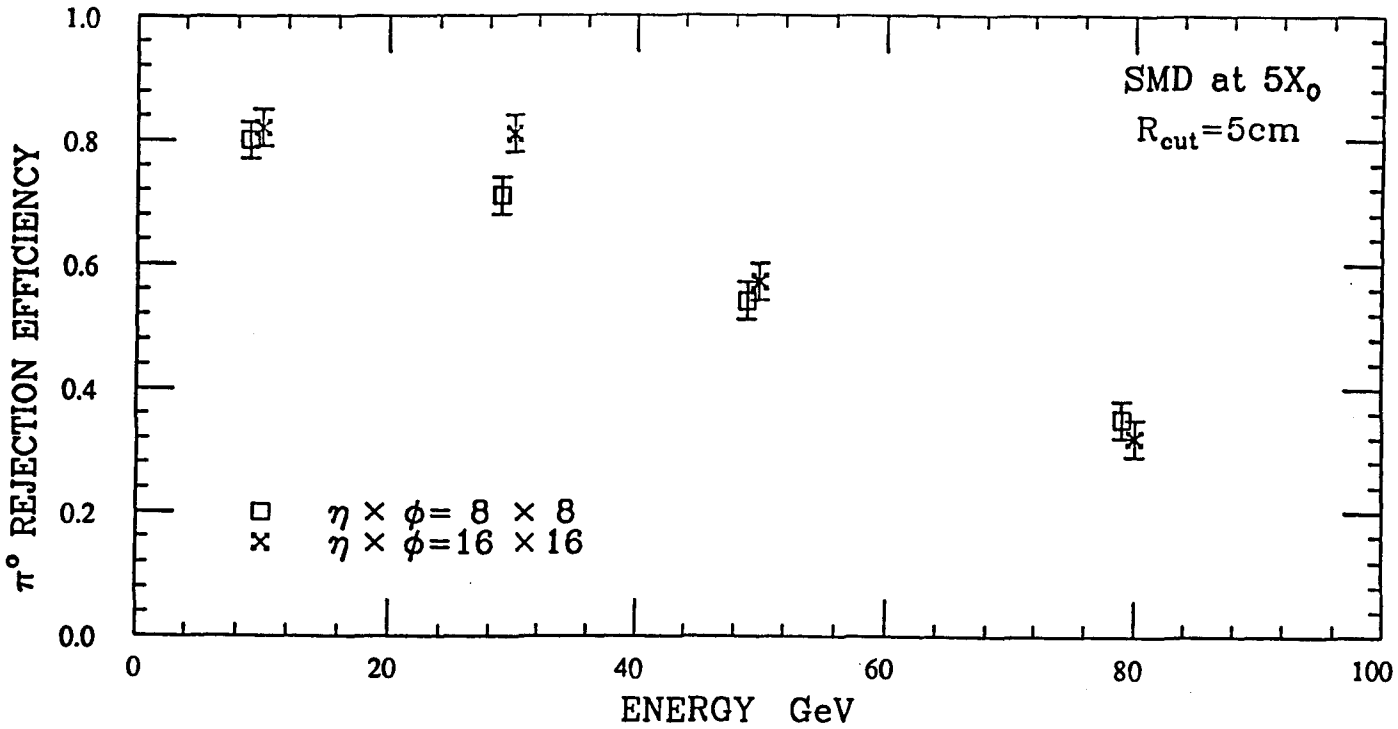
SMD at 5X0
Rcut=5cm
η × φ= 8 × 8
η × φ=16 × 16
π° REJECTION EFFICIENCY
ENERGY GeV
0.0
0.2
0.4
0.6
0.8
1.0
0
20
40
60
80
100

FIG.5a

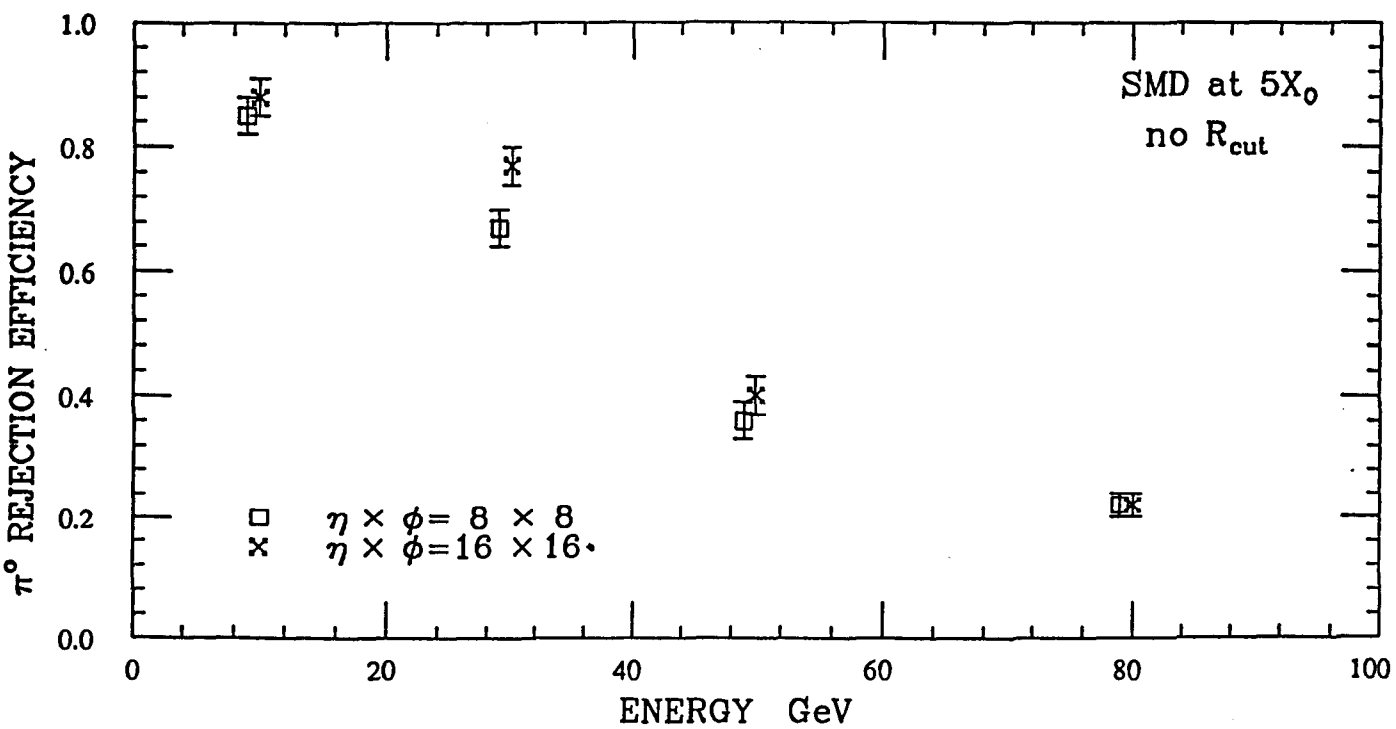
SMD at 5X0
no Rcut
η × φ= 8 × 8
η × φ=16 × 16
π° REJECTION EFFICIENCY
ENERGY GeV
0.0
0.2
0.4
0.6
0.8
1.0
0
20
40
60
80
100

FIG.5b

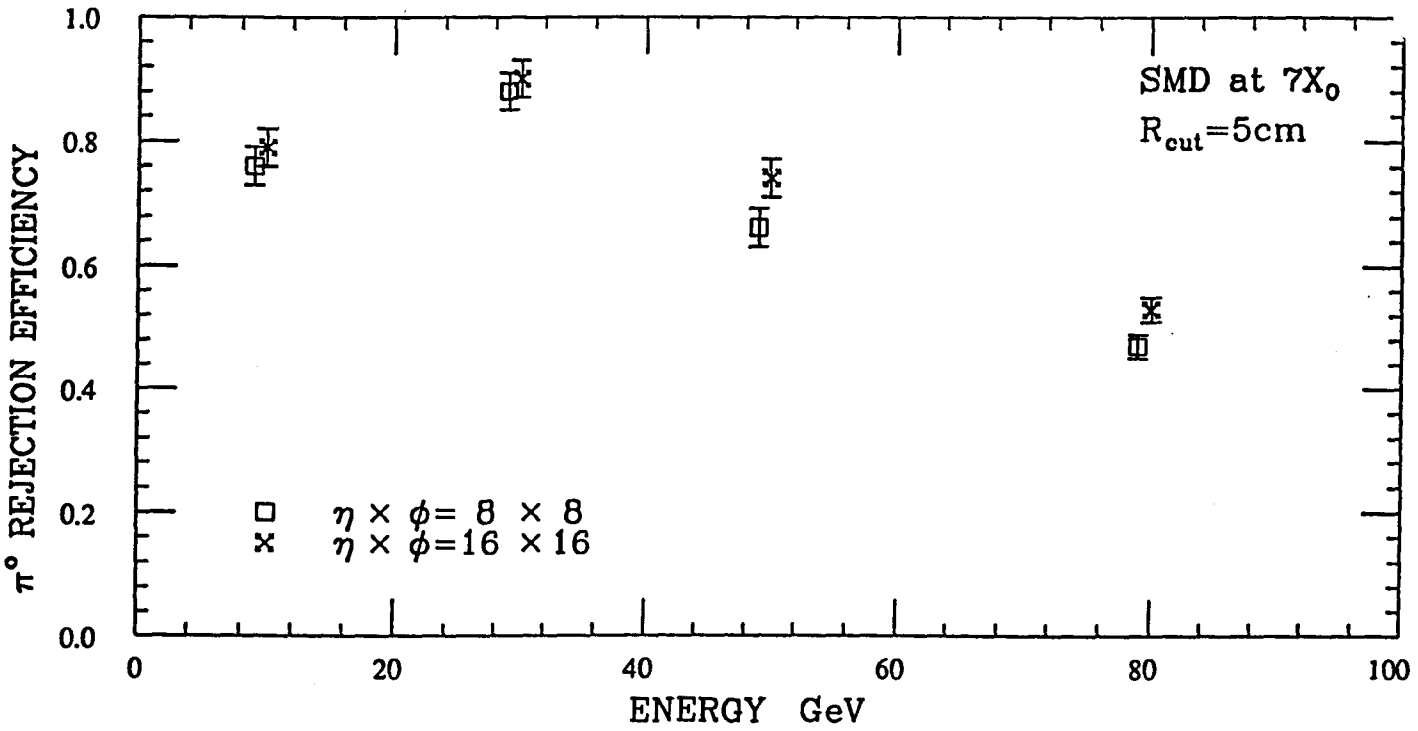
SMD at 7X0
Rcut=5cm
η × φ= 8 × 8
η × φ=16 × 16
π° REJECTION EFFICIENCY
ENERGY GeV
0.0
0.2
0.4
0.6
0.8
1.0
0
20
40
60
80
100

FIG.6a

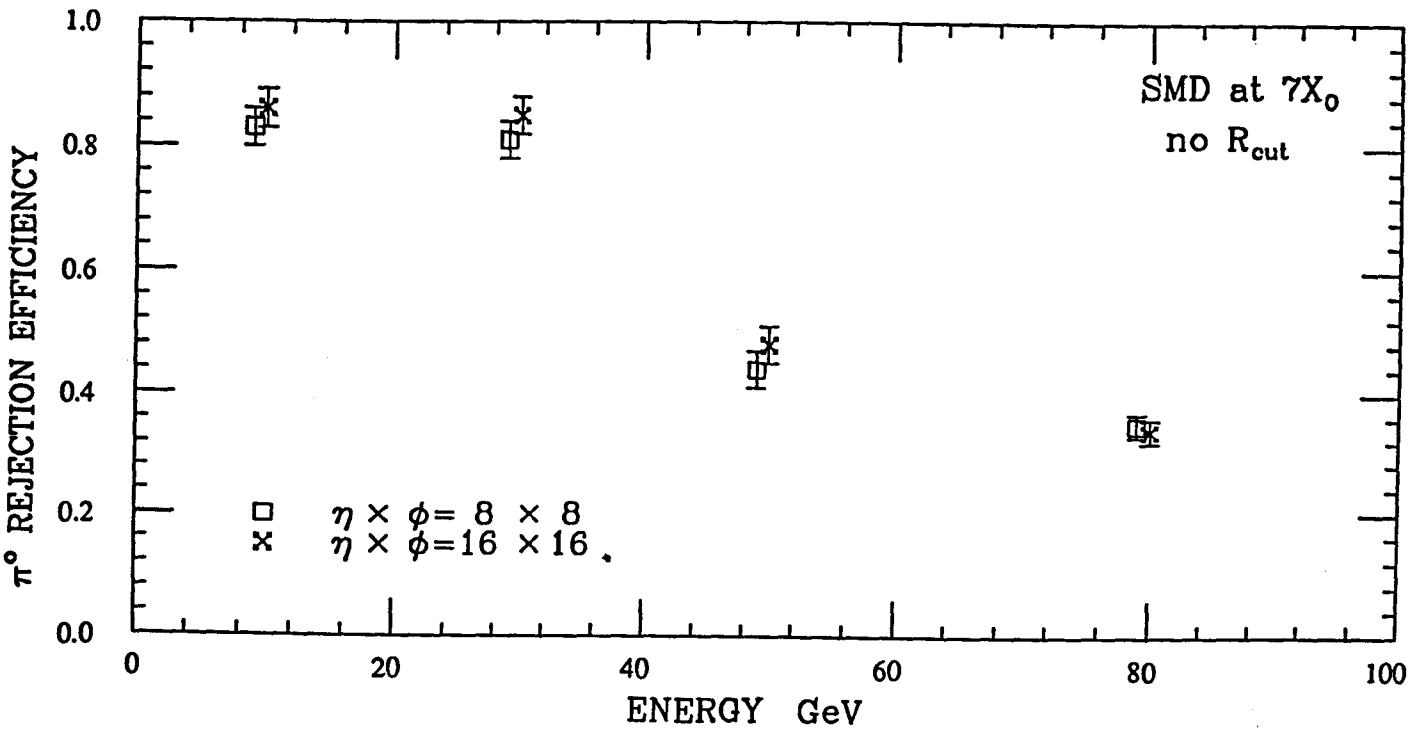
SMD at 7X0
no Rcut
η × φ= 8 × 8
η × φ=16 × 16
π° REJECTION EFFICIENCY
ENERGY GeV
0.0
0.2
0.4
0.6
0.8
1.0
0
20
40
60
80
100

FIG.6b

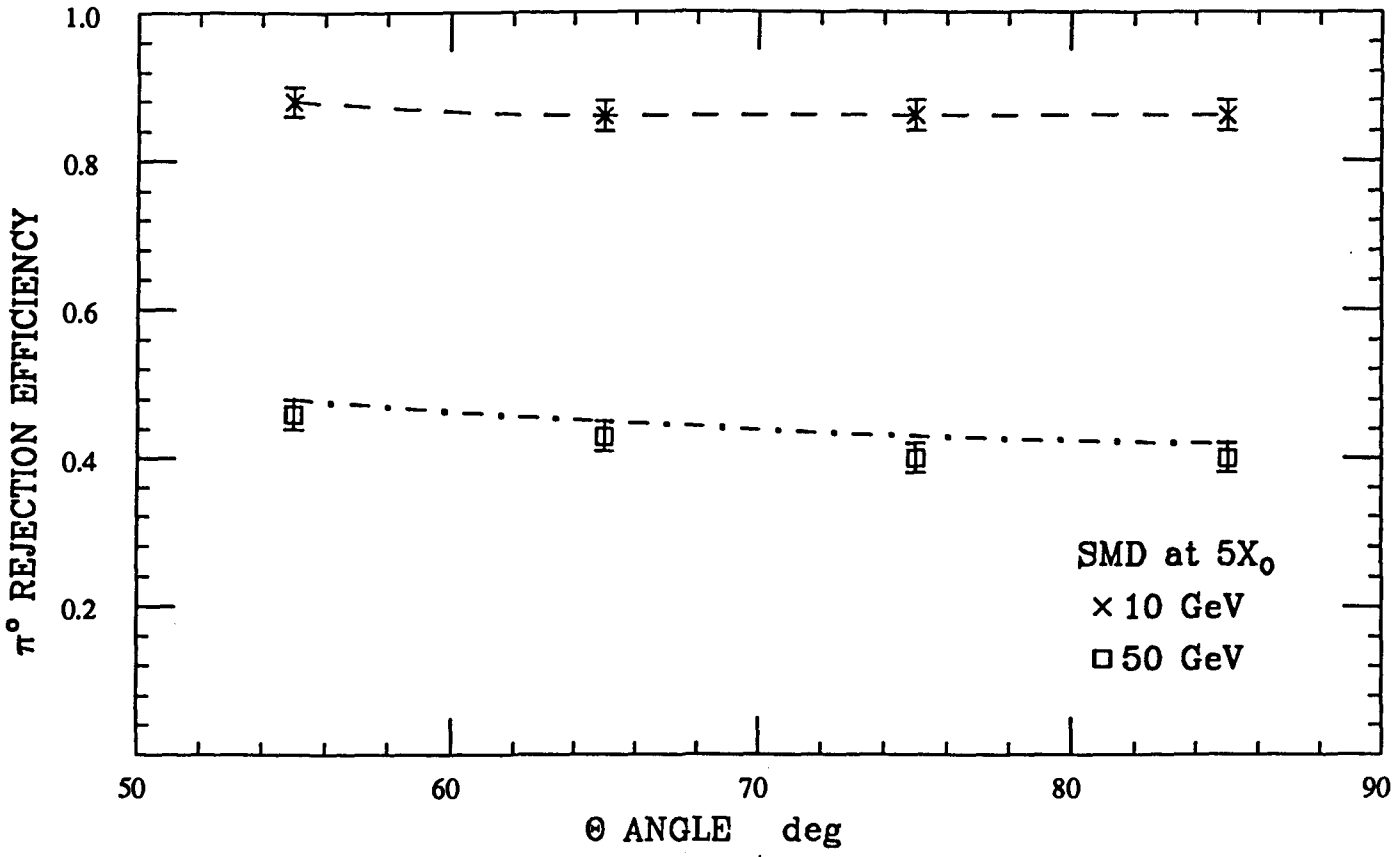
1.0
0.8
0.6
0.4
0.2
π° REJECTION EFFICIENCY
50
60
70
80
90
Θ ANGLE deg
SMD at 5X0
× 10 GeV
□ 50 GeV

FIG.7

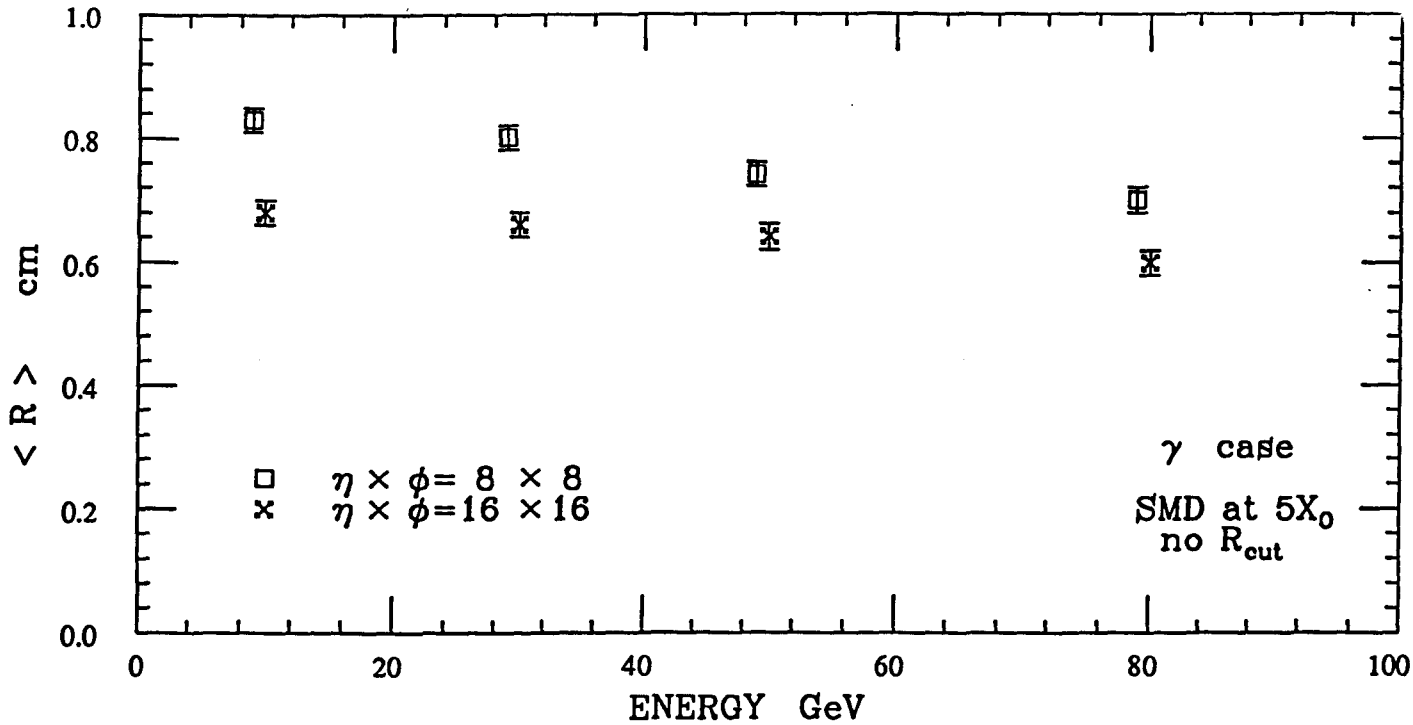
1.0
0.8
0.6
0.4
0.2
0.0
< R > cm
0
20
40
60
80
100
ENERGY GeV
η × φ= 8 × 8
η × φ=16 × 16
γ case
SMD at 5X0
no Rcut

FIG.8a

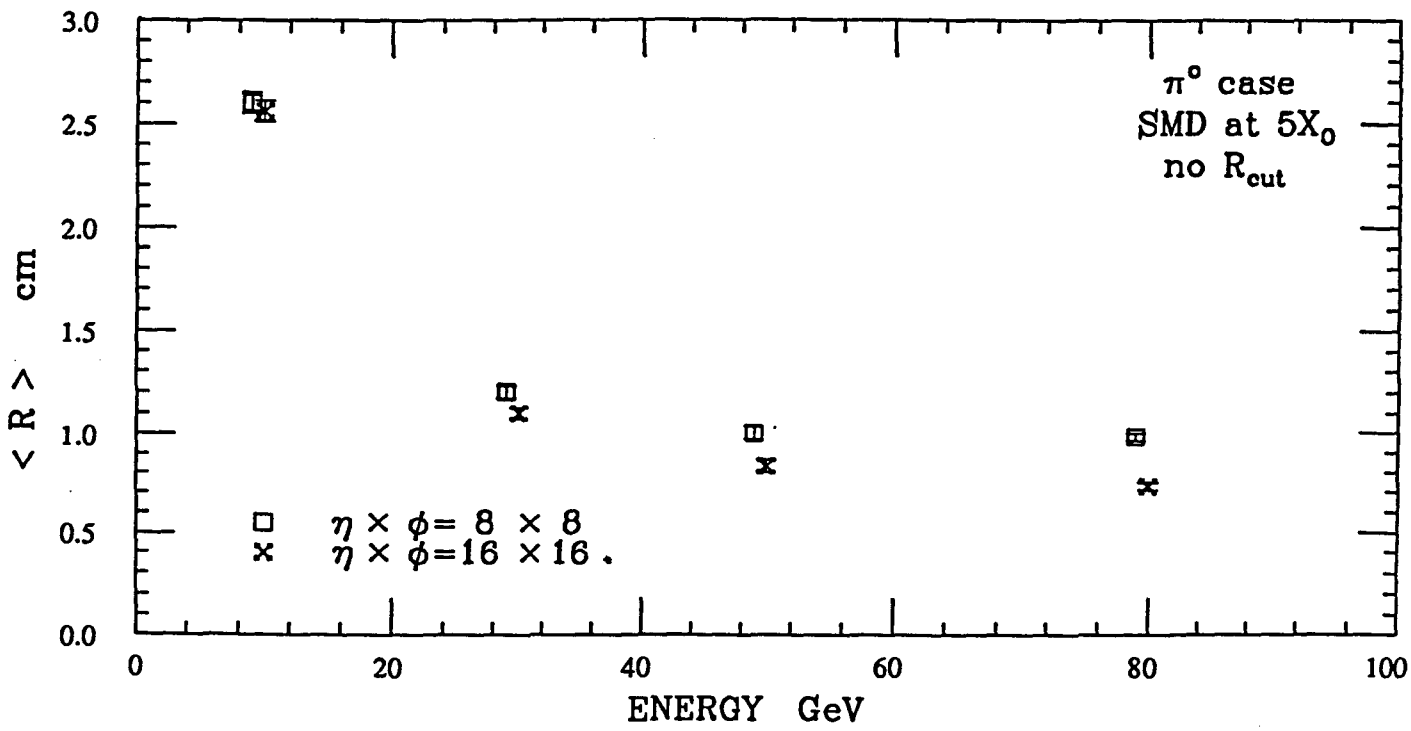
3.0
2.5
2.0
1.5
1.0
0.5
0.0
< R > cm
0
20
40
60
80
100
ENERGY GeV
η × φ= 8 × 8
η × φ=16 × 16 .
π° case
SMD at 5X0
no Rcut

FIG.8b

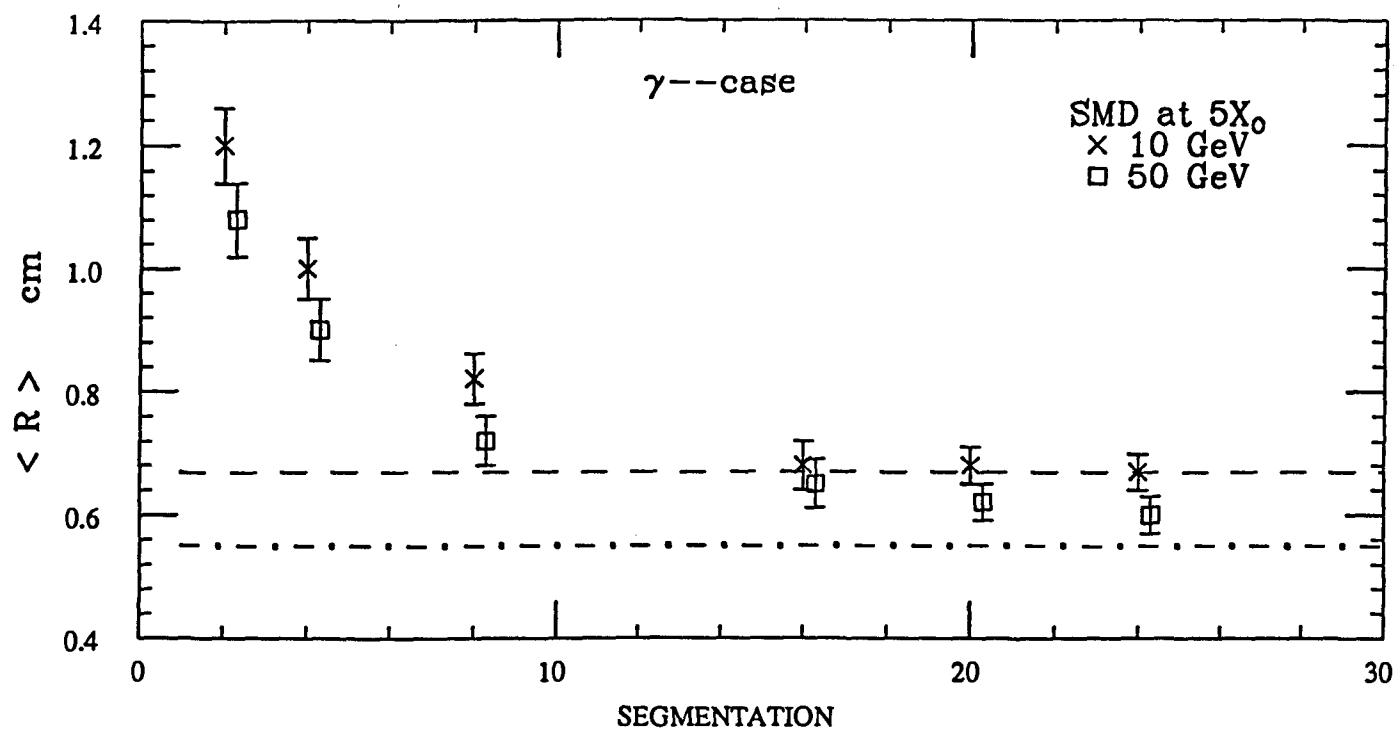
γ--case
SMD at 5X0
× 10 GeV
□ 50 GeV
< R > cm
1.4
1.2
1.0
0.8
0.6
0.4
0
10
20
30
SEGMENTATION

FIG.9a

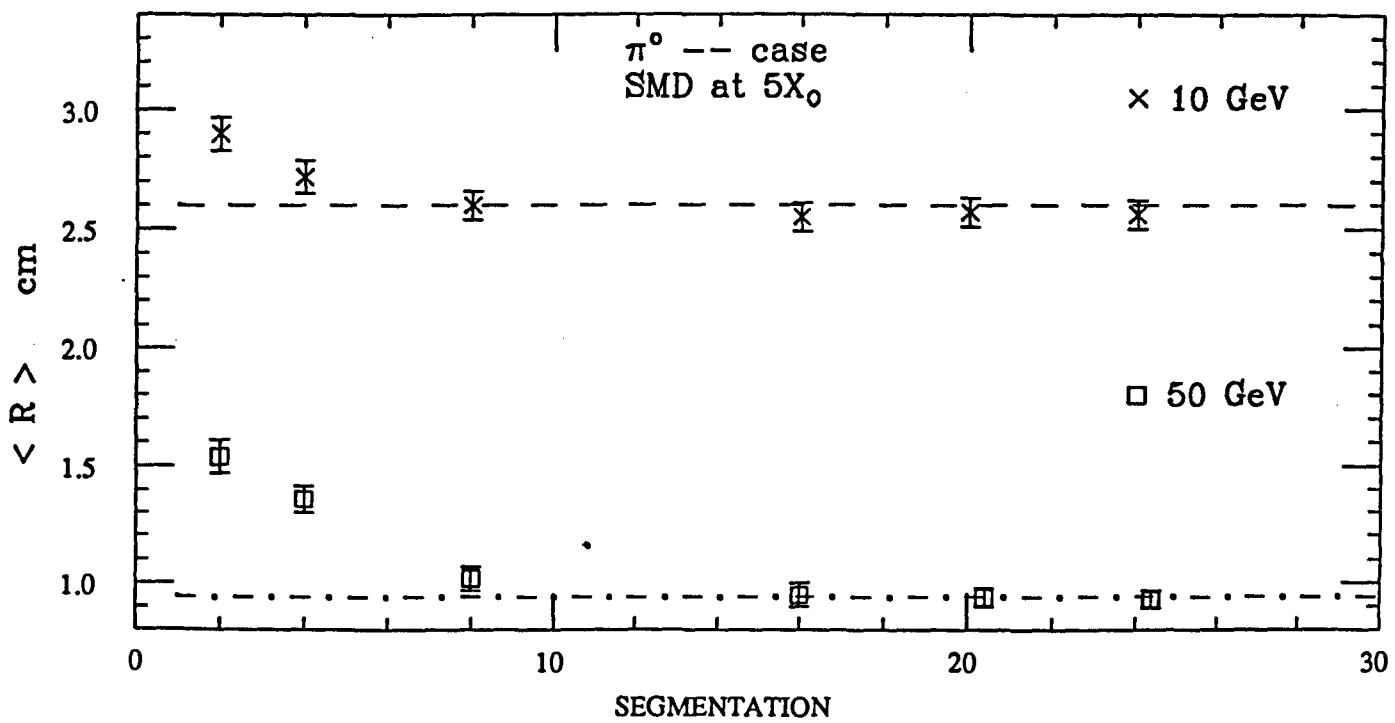
π° -- case
SMD at 5X0
× 10 GeV
□ 50 GeV
< R > cm
3.0
2.5
2.0
1.5
1.0
0
10
20
30
SEGMENTATION

FIG.9b

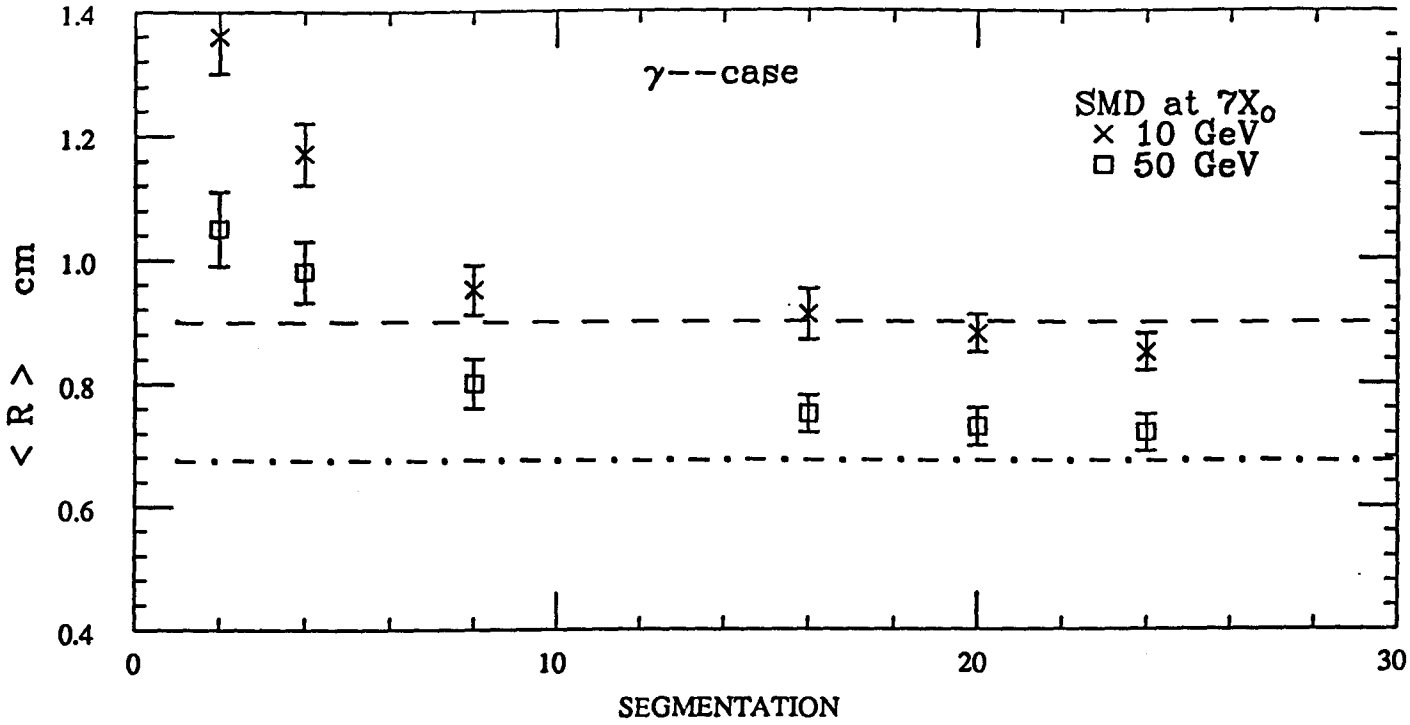

FIG.10a

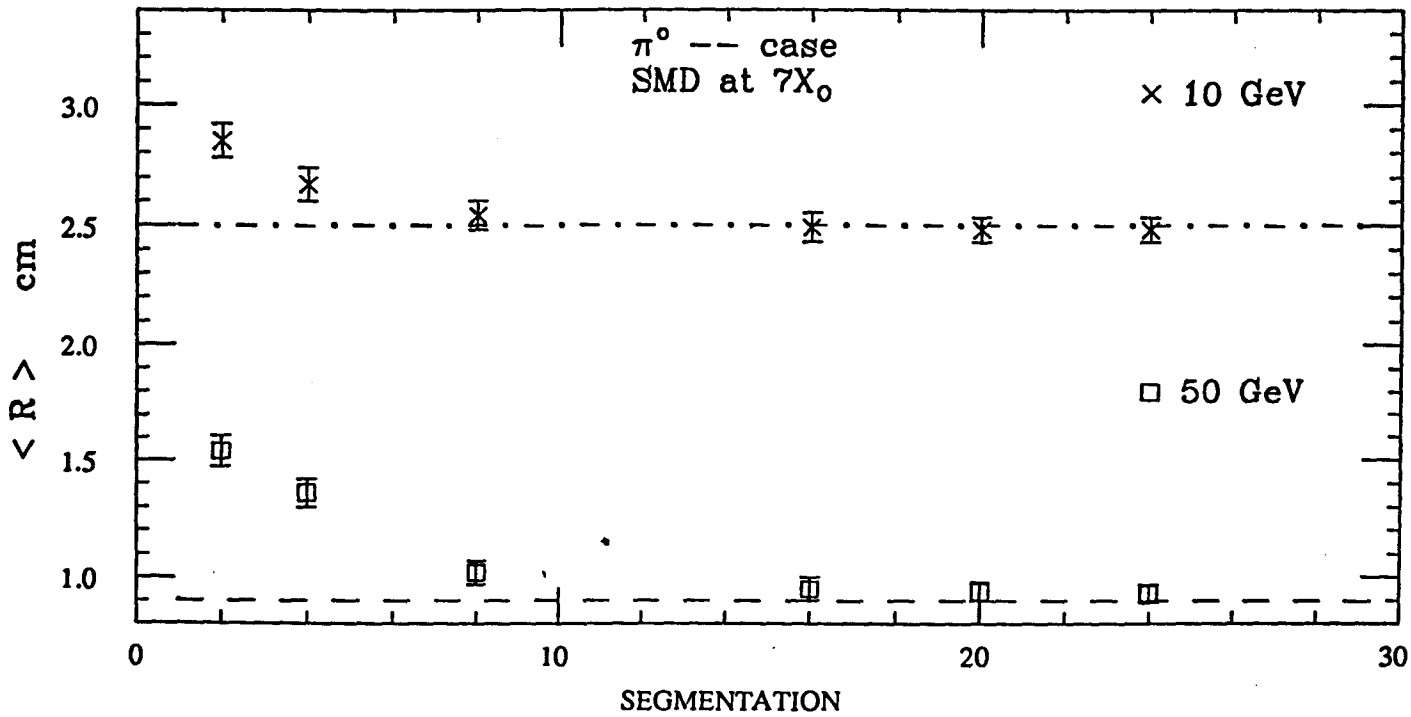

FIG.10b

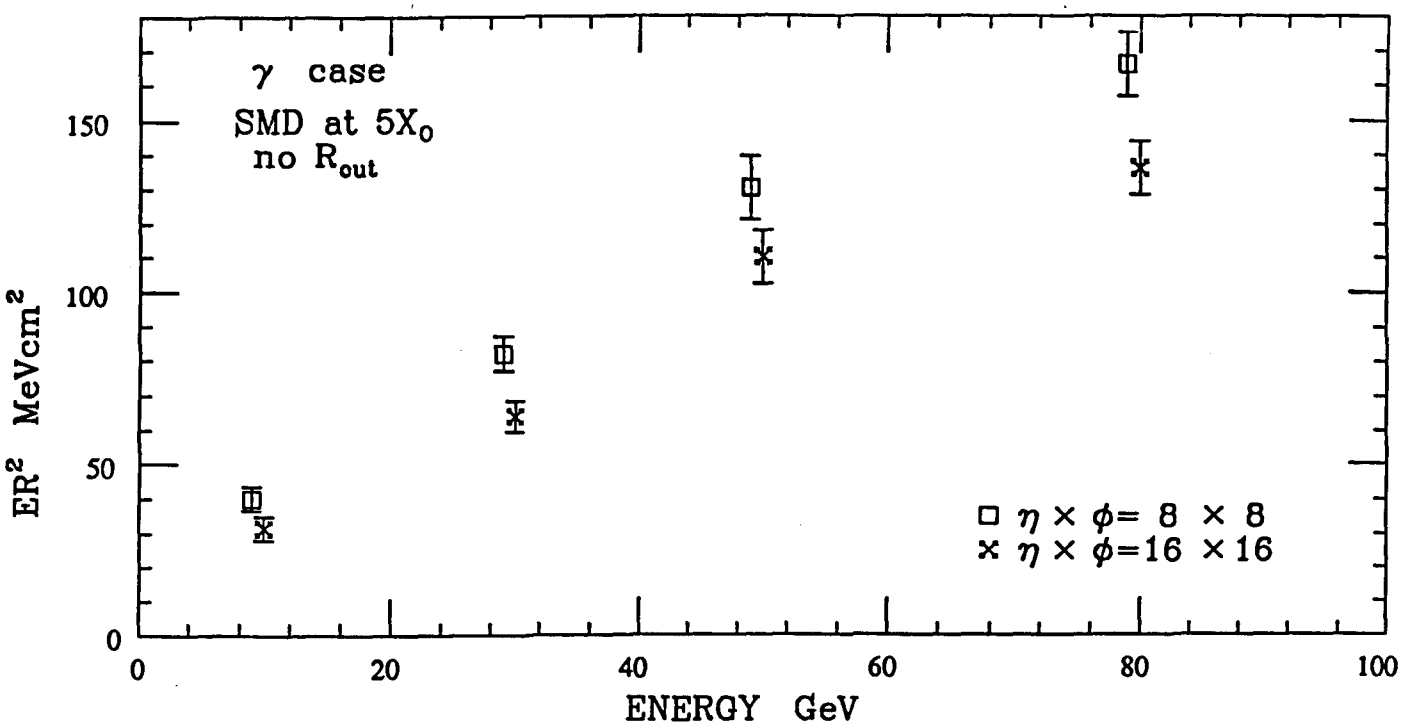

FIG.11a

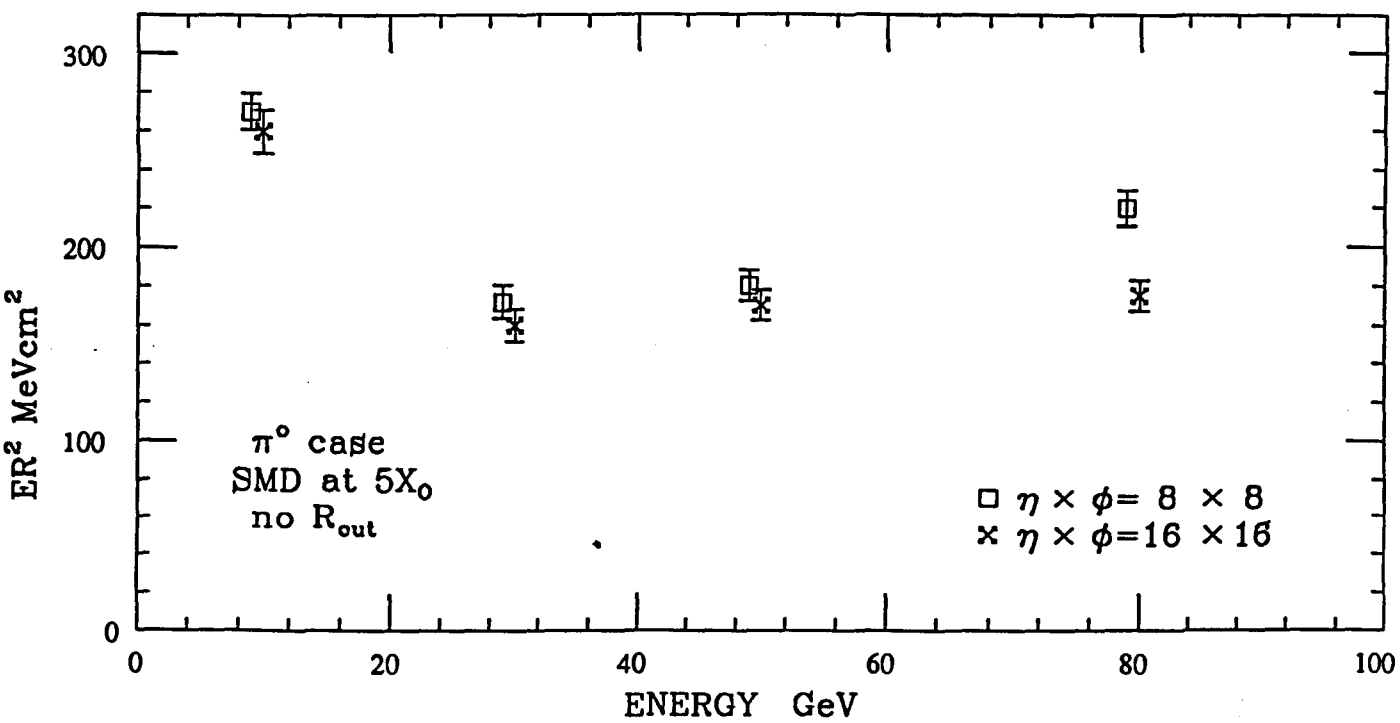

FIG.11b

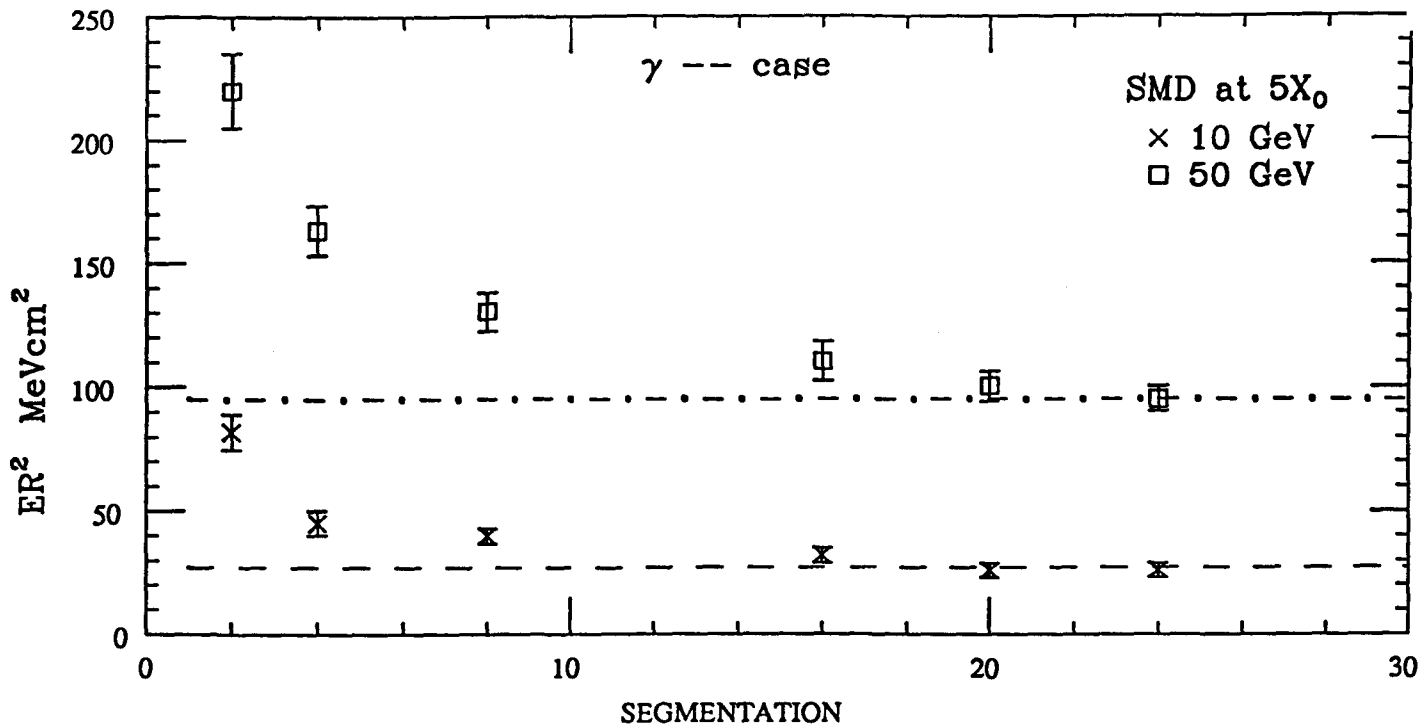

FIG.12a

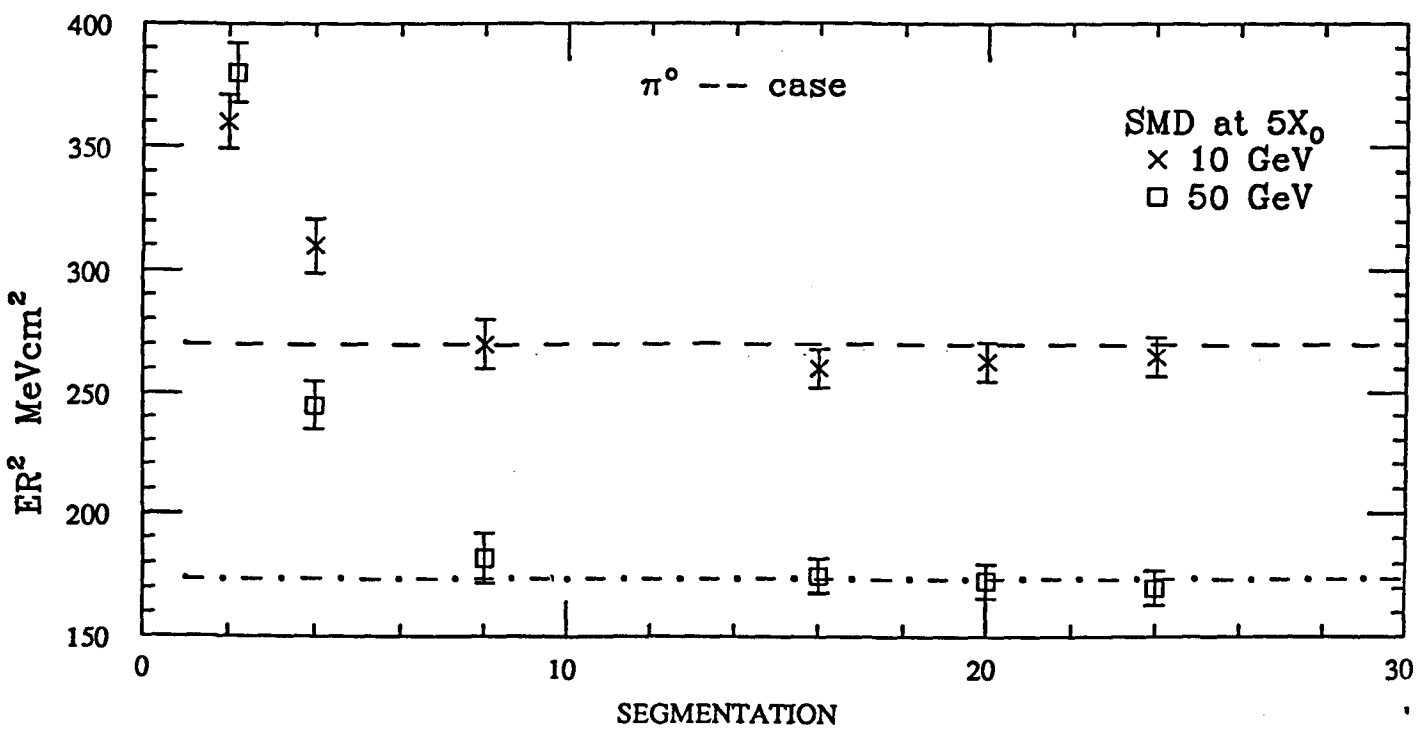

FIG.12b

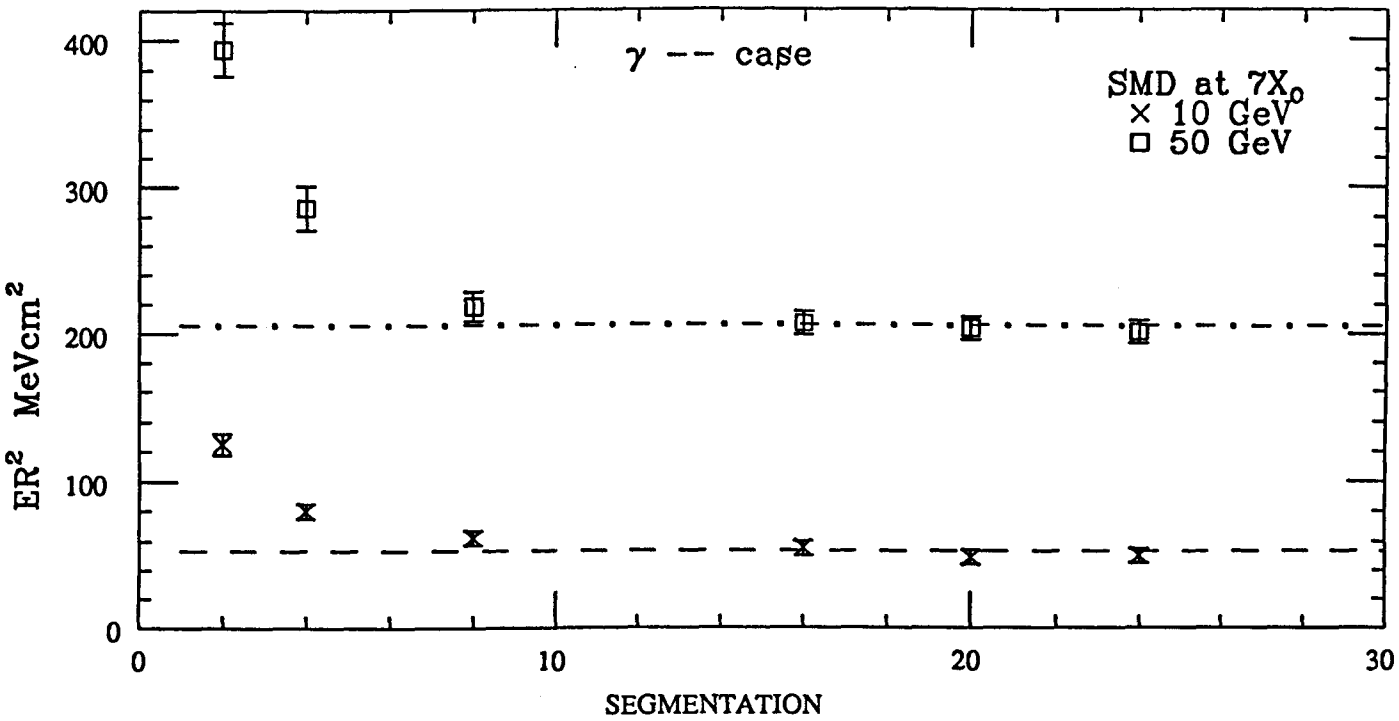

FIG.13a

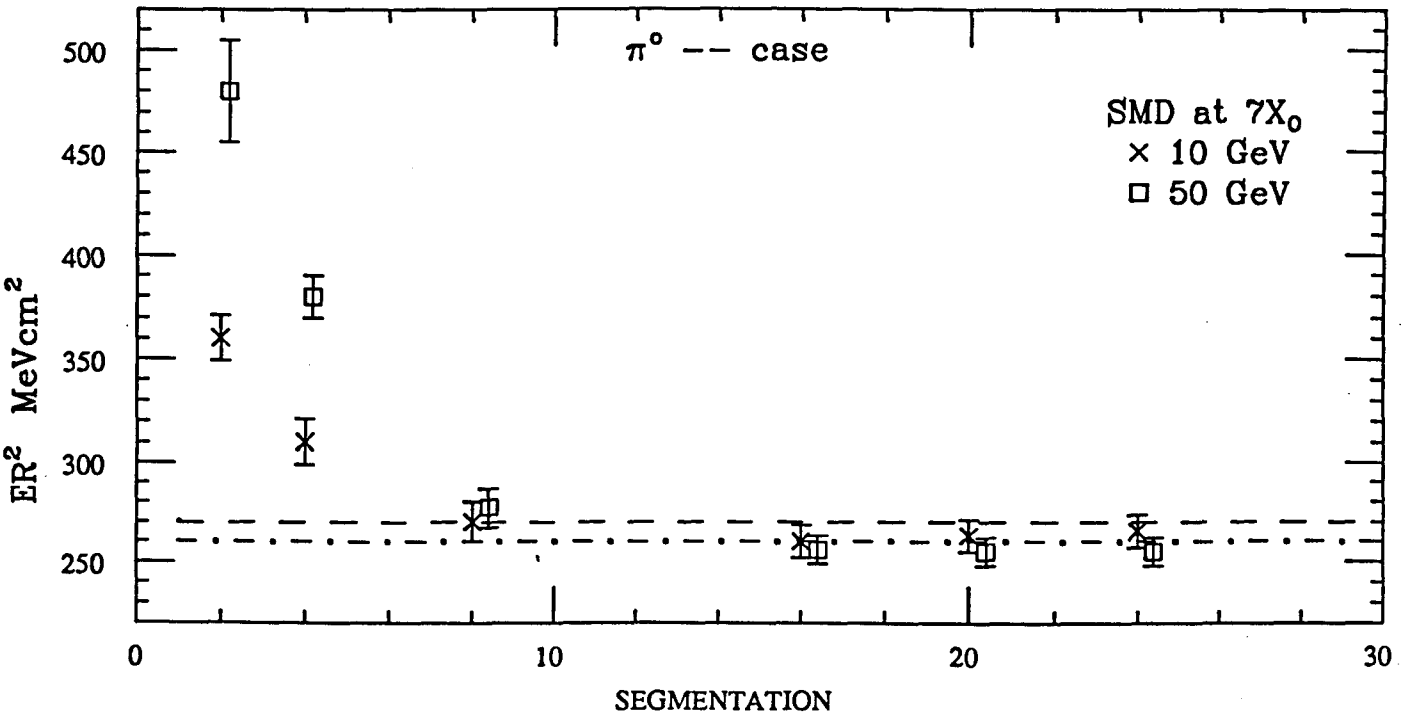

FIG.13b